Addis Ababa University

Addis Ababa Institute of Technology

School of Electrical and Computer Engineering

System Optimization and Design of Hybrid Mini Grid System Consisting of Diesel-Solar and Storage Units Using Bacteria-Foraging Algorithm: A Case Study Bohe Village-Somali Region

A thesis submitted to School of Graduate Studies, Addis Ababa Institute of Technology, Addis Ababa University in partial fulfillment of the requirement for the Degree of Master of Science in Electrical Engineering (Control Engineering)

By

Tizita Tesfaye

Advisor

Dereje Shiferaw (PhD)

February 26, 2025

Addis Ababa, Ethiopia

Addis Ababa University

Addis Ababa Institute of Technology

School of Electrical and Computer Engineering

System Optimization and Design of Hybrid Mini Grid System Consisting of Diesel-Solar and Storage Units Using Bacteria-Foraging Algorithm: A Case Study Bohe Village-Somali Region

By

Tizita Tesfaye

Approved by Examining Board

Dean, School of Graduate Committee	Signature	Date

Advisor	Signature	Date
Dr Dereje Sh		03/03/25

Internal Examiner	Signature	Date

External Examiner	Signature	Date
Dr. Mengesha Mamo		28/02/2025

Declaration

I, the undersigned, declare that this MSc thesis is my original work, has not been presented for fulfillment of any degree in this or any other university and all sources and materials used for the thesis are acknowledged.

Author

Tizita Tesfaye

Signature

_____

Place:

Addis Ababa Institute of Technology, AAiT
Addis Ababa University, AAU
Addis Ababa, Ethiopia.
Submitted by: February 26, 2025.

This thesis has been submitted for examination with the approval of my advisor Dereje Shiferaw (PhD).

Dedication

Dedicated to my family specially Mom, Dad, and my Husband.

Acknowledgment

I would like to thank God for giving me the strength and health to complete my thesis. My deepest gratitude goes to my advisor, Dereje Shiferaw (PhD), for his invaluable guidance, continuous support, and constructive feedback throughout this work.

I also appreciate the academic and administrative staff at the School of Electrical and Computer Engineering, Addis Ababa Institute of Technology, Addis Ababa University, for their support. A special thanks to my family and Ethiopian Electric Utility (EEU) for their constant encouragement and support.

Abstract

Providing a reliable and sustainable energy supply in remote and underserved regions is a significant challenge. This study presents the system optimization and optimal control design of a hybrid mini-grid system, combining diesel generators, solar photovoltaic (PV) panels, and battery storage units to meet the energy demands of Bohe Village in the Somali Region of Ethiopia. The optimization is achieved using the Bacteria-Foraging Algorithm (BFA), an advanced technique inspired by the foraging behavior of *E. coli* bacteria, ensuring the hybrid system's efficient operation in MATLAB.

The research starts by analyzing the daily load profile of Bohe Village, highlighting peak loads and total energy requirements. The hybrid system is then designed, incorporating suitable capacities for the diesel generators, PV panels, and battery storage. The BFA is applied to optimize controller gains for the inverter, boost converter, battery charging/discharging, and energy management system (EMS). The EMS dynamically selects and allocates energy sources, ensuring optimal load distribution to meet demand while preventing overloads.

The results show that the hybrid mini-grid system is well-suited for Bohe Village's energy needs. The integration of solar PV and battery storage enhances the system's sustainability and resilience against fuel price volatility and supply disruptions. This case study provides valuable insights and a framework for optimizing hybrid energy systems in similar remote locations. Ultimately, the use of BFA for hybrid mini-grid design offers a promising solution to energy challenges faced by remote communities, contributing to energy access and sustainable development.

Keywords: hybrid, photovoltaic, battery, diesel, EMS, MATLAB, BFA.

Contents

List of Figures

List of Tables

List of Acronyms

AC Alternating Current

BFA Bacterial Foraging Algorithm

BFOA Bacterial Foraging Optimization Algorithm

DC Direct Current

DG Diesel Generator

EMS Energy Management System

ESS Energy Storage System

GPS Global Positioning System

MATLAB Matrix Laboratory

MPP Maximum Power Point

MPPT Maximum Power Point Tracking

MSE Mean Squared Error

NASA National Aeronautics and Space Administration

PI Proportional-Integral

PMW Pulse Width Modulation

PV Photovoltaic

SMC Sliding Mode Control

SOC State of Charge

VSC Voltage Source Converter

List of Symbols

$P\&O$ - Perturb and Observe

KWH - Kilo Watt Hour

KW - Kilo Watt

$P_{\max}$ - Maximum Power

V_{mp} - Maximum Power Voltage

I_{mp} - Maximum Power Current

V_{oc} - Open Circuit Voltage

I_{sc} - Short Circuit Current

W - Watt

V - Volt

A - Ampere

AH - Ampere Hour

L - Load

P - Power

P_g - Power Generated

N_{pv} - Number of Solar Panels

P_r - Required Power from Solar Array

LF - Safety Factor due to Losses and Dust on the Module

N - Total Number of PV Modules

N_{series} - Number of PV in Series

N_{parallel} - Number of PV in Parallel

I_{ph} - Photo Current

I_D - Diode Current

I_s - Saturation Current

q - Electron Charge

k - Boltzmann Constant

n - Identity Factor

R_s - Series Resistance

R_{sh} - Shunt Resistance

B_c - Battery Capacity

B_{bp} - Number of Batteries in Parallel

B_{bs} - Number of Batteries in Series

D - Duty Cycle

Chapter 1

Introduction

1.1 General Background

Energy is the engine for the economic progress and development of any given society or country [1]. Access to energy is therefore a key factor in the socio-economic transformation of every country. Access of modern energy services must be reliable, affordable, sustainable and feasible with low emitting sources. Many people, particularly in the developing world, lack access to modern energy services.

Ethiopia is a country located in horn of Africa, the GPS coordinates of Ethiopia are 9.1450° N and 40.4897° E. The latitude of Ethiopia is situated in the northern hemisphere, meaning Ethiopia is above the equator. With a longitudinal coordinate in the east, Ethiopia is in the eastern region. It has a land area of about 1.1 million square kilometers and a population of 107.5 million with population growth 2.4%. Over 83% percent of the country's population is still classified as rural [2]. Ethiopian National electrification plan by 2025, 65% of access provision is targeted with grid solutions and 35% with off-grid technologies (solar off-grid and mini-grids). Bohe village (7°26'5.10"N, 46°38'37.18"E) is located in the Somali Region currently electrified with diesel mini grid and serving 154 customers for 6 hours per day and the existing capacity of Diesel generator is 375kVA.

Hybrid energy systems such as Photovoltaic (PV) cells, Diesel Generator (DG) and Energy Storage System (ESS) systems, offer the most adequate solutions for the electrification of remote areas; the combination and the ratio of the types of energy technologies

depend greatly on the resources locally available in each geographical area [3]. These resources can be evaluated only after a period of monitoring of the basic parameters such as solar radiation and temperature that are necessary for sizing and implementing renewable energy systems. Optimization of the sized photovoltaic–diesel hybrid systems guarantees the lowest investment with the use of renewable energies.

The PV solar is excellent replacements to diesel fuels because of their non-effect on the environment, but the power outputs are susceptible to variations in solar radiations [4]. Therefore, the solar radiation limits the PV solar for off-grid applications. In order to solve this problem, PV solar is hybridized with other energy technologies such as battery, diesel to ensure a continuous supply of power.

In this thesis, various control systems, including battery charging control, maximum power point tracking (MPPT) of boost, inverter control, and energy management system (EMS), are modeled and optimized using a bacteria foraging-based algorithm (BFA). MATLAB software is utilized for the system design and implementation. The integration of these advanced control strategies, along with optimization algorithms, ensures the efficient and reliable operation of the hybrid energy system, addressing the unique energy challenges of remote areas like Bohe, Somali Region, Ethiopia.

1.2 Statement of Problem

Reliable and sustainable power supply to the community living in the rural area of Bohe village, which is located far from the national grid line, is a vital problem. The challenges related to energy delivery or connection from the substation grid systems involve significant additional energy consumption and cost. Furthermore, the community follows a nomadic lifestyle, which means there is a lack of awareness and limited means of regular income generation. As a result, there is little willingness to purchase electricity, making it even more challenging to establish a sustainable energy solution.

Additionally, the availability of basic infrastructure, such as road access, telecommunication towers, health centers, and schools, requires a reliable energy supply to function effectively. However, the current energy sources in the area are primarily non-renewable,

which not only increases environmental pollution but also contributes to the depletion of natural resources. In contrast, solar energy generation is renewable and free from climate pollution, offering a cleaner and more sustainable energy solution for the community.

To address these interconnected problems, the design of an optimized hybrid mini-grid system consisting of diesel, solar, and storage units is proposed. This system optimization will be carried out using the Bacteria-Foraging Algorithm (BFOA) as a case study, aiming to create a sustainable and cost-effective energy solution tailored to the specific needs of Bohe village.

1.3 Objective of the Thesis

1.3.1 General Objective

The general objective of the thesis is to design and model an optimal control of the hybrid mini grid system which can serve the area at the least possible energy cost, better reliability and with environment friendly.

1.3.2 Specific Objectives

The specific objective are:

- To collect power demand data of the Somali region Bohe village for the design of mini grid system.
- To design an an Energy Management System control of hybrid mini grid system which consists of solar PV-diesel and storage system using MATLAB.
- To design a maximum power point tracking battery charging, and boost, and inverter control system for the solar inverter charger controller system and optimize using BFO.
- To analyze the performance of the designed system.

1.4 Methodology

The basic procedures to complete the thesis and meet specified objectives of thesis are shown in the following flowchart, 1.1.

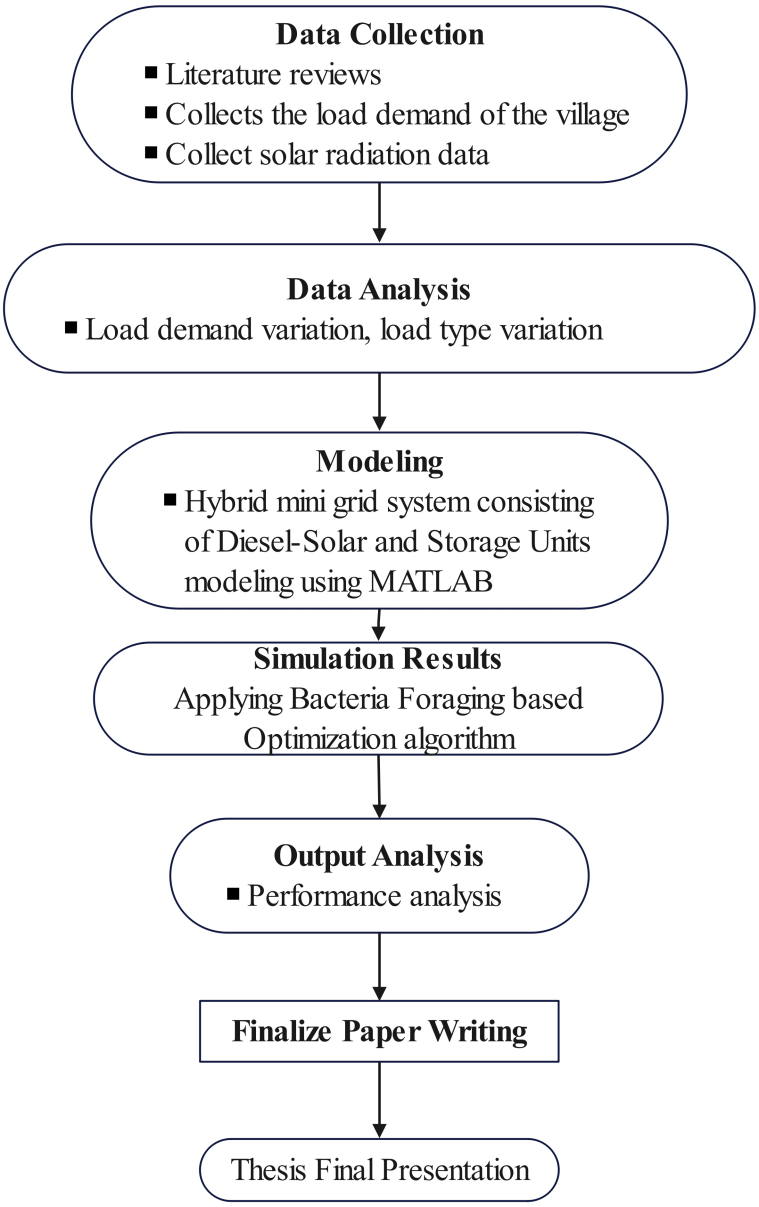

Figure 1.1: Research Methodology

1.5 Significance of the Thesis

The significant contributions of the thesis are:

- Provides a solution for meeting energy requirements in remote areas like Bohe Village, Somali Region, where access to reliable electricity is limited.
- Offers an optimal design for a hybrid mini-grid system, integrating diesel, solar, and storage units to ensure continuous power supply while minimizing environmental impact.
- Introduces the use of the Bacteria-Foraging Algorithm (BFA) for system optimization, showcasing its effectiveness in finding optimal solutions for complex energy systems.
- Validates the proposed approach through a case study in Bohe Village, Somali Region, demonstrating its practical applicability and effectiveness in real-world scenarios.
- Contributes to the promotion of sustainable energy practices by reducing reliance on fossil fuels and maximizing the utilization of renewable energy sources.
- Aims to minimize the operational costs associated with electricity generation and distribution, thereby improving affordability and accessibility for local communities.
- Offers insights and methodologies that can be replicated in similar off-grid or underserved regions worldwide, fostering global efforts towards energy access and sustainability.

1.6 Scope and Limitation of Thesis

This thesis focuses on hybrid mini grid system design consisting of diesel, solar and storage units. The various system components are modeled and bacteria foraging based optimization algorithm is used for the maximum power point tracking control of battery charging control and overall system optimization. In the overall system design MATLAB

software was used. The design system utilized on Somali Region Bohe village as a case study. The thesis is limited to the following conditions:

- Findings and recommendations are tailored to the unique geographical and socio-economic conditions of Bohe Village and mayn't be directly applicable to all regions.
- The effectiveness of the proposed solution is influenced by the availability and reliability of technology, which can vary depending on the region.
- The scope of the study limited by the availability of resources such as data, funding, and expertise, which affect the depth and breadth of the analysis.
- Energy systems are subjected to technological advancements, policy changes, and evolving socio-economic factors, which impact the long-term viability of the proposed solutions.
- Practical implementation of the proposed hybrid mini-grid system face challenges related to infrastructure, regulatory frameworks, and community engagement.

1.7 Thesis Outline

The thesis outline is organized into six chapters. Chapter 1 provides a general introduction to hybrid mini-grid system modeling and control. Chapter 2 discusses a review of various research papers related to the thesis. Chapter 3 presents the hybrid mini-grid system, consisting of diesel-solar and storage units, including modeling and overall sizing. Chapter 4 introduces the Maximum Power Point Tracking (MPPT) and Proportional Integral (PI) control scheme design for battery charging control and system optimization. Chapter 5 discusses the simulation results and provides an analysis based on these simulations. Finally, Chapter 6 draws conclusions from the overall analysis performed and offers recommendations for future work.

Chapter 2

Literature Review

In Ethiopia, hybrid power generation system, and rural electrification, literature study was essential. Various literature and thesis studies have been conducted on Hybrid mini grid system consisting of Diesel-Solar and storage units. Several researches have been done on the area of hybrid system since long time and numerous research results for a variety of applications have been published. Some of these are presented as follows.

Getachew Bekele et al. (2012), proposed design of the hybrid wind and photovoltaic power generation system for the Ethiopian remote area [5]. The research studies design the system for basic electrification requirement. The data for the study collected from national agency. The simulation of that hybrid system was analyzed by using the HOMER software. The results of the study was concluded with satisfied working of the system and the shortage of electricity was covered up to 20%.

Feyisa Bekele (2017) explored the optimal sizing of renewable small power plants, including solar, hydro, and diesel systems, using HOMER software based on economic criteria [6]. However, the study did not utilize the MATLAB Simulink environment for designing DC-DC converters or developing an energy management system algorithm. To fill this gap, the present study aims to incorporate more efficient methods for optimal sizing, along with the design of DC-DC converters and energy management algorithms using the MATLAB Simulink environment. By leveraging the advanced capabilities of these tools, this study seeks to provide a more comprehensive and effective approach to determining the optimal sizing of renewable small power plants.

Lie Xu et al. (2011) presented a technique for controlling and operating DC voltage in systems with variable generation and energy storage [7]. However, their approach was unable to achieve effective power coordination between batteries, diesel generators, and electrolyzers. To overcome this limitation, the study proposes the use of an efficient interleaved DC-DC converter, along with MATLAB function code and a fuzzy controller with carefully defined linguistic variable ranges. This combination facilitates proper power coordination among solar, wind, battery, and DC loads.

Malla et al. (2014) focused on load shedding and DC-link voltage control, using battery state of charge and a PI controller, respectively [8]. However, this study enhances the energy management system by using both battery state of charge and power difference as inputs. Additionally, a PSO-tuned PID controller is preferred for more effective DC-link voltage control, improving overall system performance.

Halim et al. (2018), proposed a research titled 'Review on Optimised Configuration of Hybrid Solar-PV Diesel System for Off-Grid Rural Electrification' in order to supply a 24 hours of uninterrupted power to the settlement [9]. The hybrid solar-PV diesel energy system was one of the most reliable, cost –efficient, and environmentally friendly system that can serve remote areas, where the diesel generator acts as a backup solution in the absence of solar radiation or at night. The annual emission was amounting at 432259 kg from standalone diesel generator, while hybrid system produced emissions of 342246 kg show on hybrid solar-PV diesel systems implemented with the economical outcome using the HOMER software.

Hussein et al. (1955), has developed a new Maximum Power Tracking (MPT) algorithm to track Maximum Power Operating Point (MPOP) by comparing the incremental and instantaneous conductance of the PV array [10]. The drawbacks of Perturb and Observe method were analyzed and it showed that the Incremental Conductance algorithm has successfully tracked the MPOP even when atmospheric conditions changes rapidly. The work was carried out by both simulation and graphs.

Abdelhaq Bensaber et al. (2019) investigated power flow management in hybrid power systems and proposed the use of a fuzzy logic controller to meet load demands [11]. Their approach, however, encountered a limitation when the load power exceeded

the available generated power and the battery reached its minimum state of charge. In such instances, the battery would only begin charging once all loads were disconnected. To address this issue, the study suggested a potential solution: temporarily disconnecting less critical loads until the total load power falls below the generated power, allowing for simultaneous battery charging.

M. Nagaiah et al. (2020) analyzed a bi-directional DC-DC converter controlled by fuzzy logic for managing battery energy in a solar-wind hybrid microgrid system [12]. However, their approach did not incorporate load prioritization based on the state of charge and power differentials, which is crucial for ensuring uninterrupted power to critical loads. Additionally, the bi-directional converter used in their study exhibited lower efficiency. As a result, the performance of hybrid systems can be further improved by implementing a load prioritization mechanism and adopting a more efficient interleaved bi-directional converter.

Addis Ayalsew (2020) proposed a fuzzy logic controller for maximum power point tracking in a hybrid solar-wind power generation system [13]. However, his study employed conventional methods for determining the optimal sizing of the hybrid system components and did not integrate an energy management system to enhance system reliability and stability. To address this shortcoming, this paper aims to implement PSO-based optimal sizing of hybrid system components along with an efficient energy management system utilizing multiple decision variables. This approach will be realized through both MATLAB function code and fuzzy logic controllers to improve the overall system performance.

Yimen et al. (2018), proposed a method about the analyzing of a photovoltaic-wind-biogas-pumped-hydro off-grid hybrid system for rural electrification in Sub-Saharan Africa—case study of Djoundé in Northern Cameroon [14]. Traditional electrification methods, including grid extension and stand-alone diesel generators, have shown limitations to sustainability in the face of rural electrification challenges in sub-Saharan Africa (SSA), where electrification rates remain the lowest in the world. This study aims at performing a techno-economic analysis and optimization of a pumped-hydro energy storage based 100%-renewable off-grid hybrid energy system for the electrification of Djoundé,

which is a small village in northern Cameroon. Hybrid Optimization of Multiple Energy Resources (HOMER) software was used as an analysis tool, and the resulting optimal system architecture included an 81.8 kW PV array and a 15 kW biogas generator, with a cost of energy (COE) and total net present cost (NPC) of €0.256/kWh and €370426, respectively.

Micro-grids consist of clusters of loads, storage systems, and distributed generators that operate as a single or multiple controllable systems. Distributed Generation (DG) in micro-grid operations offers multiple benefits to utility operators, DG owners, and consumers, including reliable power supply, reduced need for transmission system expansion, and increased renewable power penetration [4]. Energy storage devices are a major component of micro-grids and are critical for their successful operation. These devices balance power and energy demand with generation in typical micro-grid applications.

Currently, various types of rechargeable batteries are used as energy storage devices, including Lead-acid, Nickel-cadmium, Nickel-metal hydride, Lithium-ion, Lithium-polymer, and Zinc-air batteries. To determine the optimal battery type, important attributes to consider include specific energy, service life, load characteristics, price, safety, self-discharge rate, environmental impact, and disposal methods. Nickel-cadmium, Nickel-metal hydride, and Lithium-ion batteries are often used in critical and extreme temperature applications [4, 15]. Hence the system design incorporates different types of converters, such as Boost DC-DC converters, buck-boost converters, inverters, and buck converters, to interface with system modeling [16, 17].

Maheri et al. (2014) proposed two algorithms for multi objective optimization in wind-PV-diesel generator based system [18]. In one scenario, most reliable system was created under cost constraint and in second scenario, the most cost-effective system was obtained under reliability constraint.

Electricity access in refugee camps is often limited to critical operations for humanitarian agencies and is typically powered by fossil fuel generators. This reliance on diesel generators leads to high operational costs and significant environmental impact. Studies have explored the economic and environmental benefits of optimized fully renewable and diesel-hybrid mini-grid designs in humanitarian settings. These studies aim to displace

diesel use and thereby reduce both costs and emissions. One case study of Nyabiheke camp in Rwanda demonstrates the substantial benefits of such systems [19]. The study found that optimized hybrid mini-grid designs can achieve savings of up to 32% in total costs and an 83% reduction in emissions, with cost payback times ranging from 0.9 to 6.2 years. These savings are significant and demonstrate the potential for hybrid systems to provide economic and environmental benefits over traditional diesel systems.

Solar diesel hybrid mini-grid design considerations: Bangladesh Perspective have been studied by Yusuf et al. [20]. With the decreasing cost of solar PV panels and the rising cost of diesel, solar PV systems have become increasingly popular for rural electrification. Rural areas typically exhibit minimal electricity demand with sparse distribution of loads, making it economically impractical to extend national grid lines to remote off-grid regions. One significant challenge in developing minigrids is managing the storage systems effectively. Integrating a small diesel generator not only reduces the dependency on storage systems but also ensures energy availability during periods of low solar insolation.

Chapter 3

Design of Hybrid Mini Grid System Consisting of Diesel-Solar and Storage Units

3.1 Working Principle and Basic Definitions

The overall structure of the hybrid system includes solar and diesel energy sources, battery storage, and power electronics. Each component has a specific function and will be modeled using MATLAB R2024a Simulink environment. The solar panel generates electricity from sunlight while the diesel generator converts chemical potential energy from the diesel. The battery acts as a buffer, storing excess energy for later use.

The modeling and design of a hybrid mini-grid system consisting of diesel-solar, storage units, inverters, and Maximum Power Point Tracking (MPPT) charge controllers involves a comprehensive approach to ensure efficient and reliable energy supply. The process begins with meticulous modeling, where various factors such as energy demand patterns, solar irradiance data, and diesel generator performance are analyzed to determine the optimal configuration of the system components [20, 21].

In this sequence, the solar panels serve as the primary source of renewable energy, converting sunlight into electricity through photovoltaic technology. However, solar power

generation is inherently variable due to weather conditions and time of day. To address this variability, storage units, typically batteries, are integrated into the system. During periods of high solar generation, excess energy is stored in the batteries for later use when solar output is low and demand exceeds generation capacity.

The diesel generators complement the solar power generation by providing backup power during periods of high energy demand and failure to work with the solar power condition [19, 22]. These generators are equipped with automatic controls that start and stop them based on the system's energy needs, ensuring efficient operation and fuel consumption. The integration of diesel generators enhances the reliability of the mini-grid system, particularly in remote area of Boohe Wereda, Somali, Ethiopia.

Inverters play a crucial role in the hybrid mini-grid system by converting the direct current (DC) electricity generated by the solar panels and stored in the batteries into alternating current (AC) suitable for use in homes, businesses, and industries connected to the grid [23, 24]. Inverters often include power management features to optimize energy flow within the system, ensuring maximum efficiency and stability and, this is the case where it determines exactly the working source for the current load demand and will be discussed in this thesis in the following sections.

A hybrid controller serves as energy management system which manages the distribution of power between the solar panels, batteries, and diesel generator. It optimizes the use of solar energy and minimizes the reliance on diesel fuel, thereby reducing operational costs and environmental impact [25].

Maximum Power Point Tracking (MPPT) charge controllers enhance the performance of the hybrid mini-grid system by continuously monitoring and adjusting the voltage and current from the solar panels to operate at their maximum power point. This optimization maximizes the energy harvest from the solar panels, improving overall system efficiency and reducing reliance on diesel generators. Through careful modeling and design, the integration of these components in a hybrid mini-grid system ensures reliable, cost-effective, and environmentally sustainable energy supply to Boohe communities, contributing to energy access and socio-economic development is heavily assessed in this thesis.

The photovoltaic (PV) power market is rapidly expanded due to the rapid growth

in renewable energy sources, especially in distributed generation field and hence, the remote area of Boohe village is considered as a case study. So, the PV designs are needed tobe a reliable and flexible tool to provide the power generation by the PV systems of various sizes and system components. By the use of solar system: solar cell, panel, and photovoltaic array, storage devices, inverters, MPPT storage charge controllers, and diesel system the mini-off grid system is designed in the following sections.

Solar cell is an electronic device that converts the energy of light directly into electricity by the photovoltaic effect. Solar panel is actually a collection of solar (photovoltaic) cells, which can be used to generate electricity through photovoltaic effect. Photovoltaic array is therefore multiple solar panels electrically wired together to form a much larger PV installation (PV system) called an array.

The equivalent circuit of a PV cell is shown in Figure 3.1 and further explained in Figure 3.8. The current source I_{ph} represents the cell photocurrent, R_{sh}, and R_s are the intrinsic shunt and series resistances of the cell, respectively. Usually the value of R_{sh} is very large and that of R_s is very small, hence they may be neglected to simplify the analysis. Practically, PV cells are grouped in larger units called PV modules and these modules are connected in series or parallel to create PV arrays which are used to generate electricity in PV generation systems.

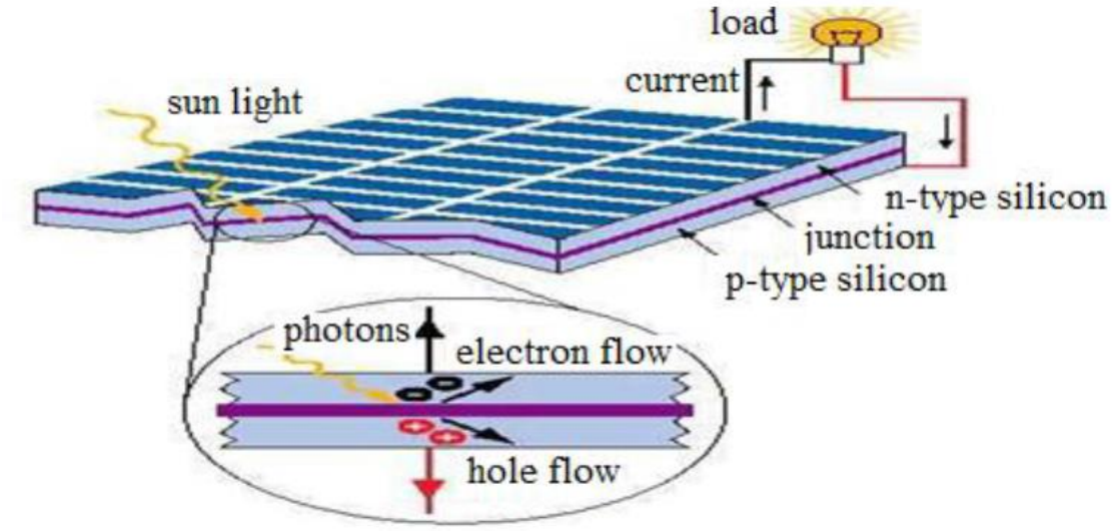

Figure 3.1: Typical PV Cells Energy Conversion [15]

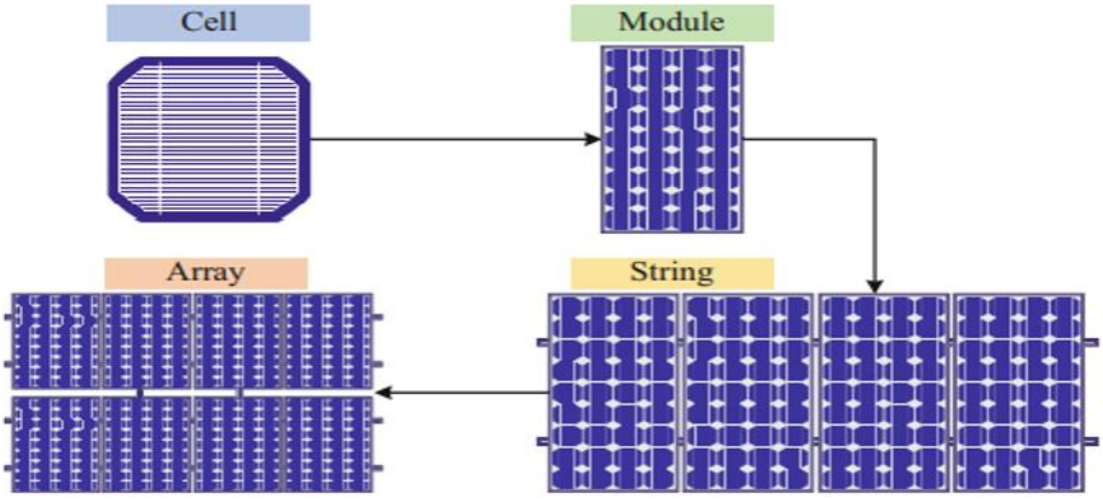

Figure 3.2: Schematic Diagram of a Solar Cell to Array [15]

To create a PV module, PV cells need to be combined, and then these modules are further combined to create PV panels or arrays. The number of PV cells in a module can vary from 36 to 96, and their sizes may also vary [16]. The cells can be connected either in series or parallel, based on the load requirements. Just like cells, modules can be combined in series or parallel configurations. For instance, PV cells can be connected in parallel to generate high output current, and in series to generate high output voltage. Similarly, solar panels can also be combined in a series-parallel arrangement to create the desired PV array [16].

3.2 Solar System Design

The solar system design has a major system components called solar PV system which includes different components that should be selected according to the system type, site location and applications. This is constructed in the following subsections.

3.2.1 Site Location and Appliance Selection

Every solar system design starts from site location and appliance (load) selection. This phase is usually called data collection and analysis. Hence, Boohe Wereda, Somali region, Ethiopia is selected as the specified case study area of site location. The geographical

location of Boohe is given by the Latitude of 7.4362°, longitude of 46.6471°, and elevation of 518.12 meters. After selecting the desired site location the next phase is selection of the required available data of solar irradiance for Boohe. Therefore, yearly average of monthly irradiance data for Boohe is taken from 2011 to 2020 in kWh/m2/day taken from National Aeronautics and Space Adminstration (NASA), Table 3.1.

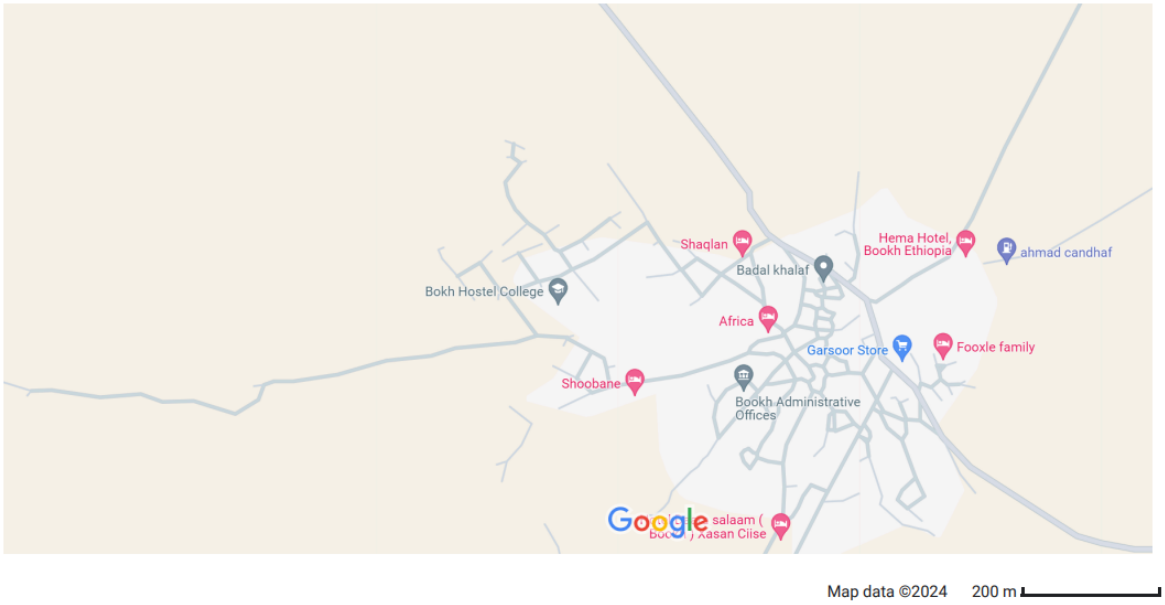

Figure 3.3: Geographical Location of Bookh

Table 3.1: Yearly average of Monthly Irradiance for Boohe 2011-2020 kWh/m2/day (Source: NASA)

Year	Jan.	Feb.	Mar.	Apr.	May	June	July	Aug.	Sep.	Oct.	Nov.	Dec.
2011	6.59	7.13	7.50	6.67	6.11	5.71	5.18	6.32	6.16	6.10	5.93	6.31
2012	6.53	7.06	7.31	6.55	6.26	5.92	5.34	6.41	6.33	6.04	6.15	6.06
2013	6.31	7.03	6.39	6.25	6.71	5.08	4.89	6.36	6.72	5.83	6.05	6.42
2014	6.66	6.97	6.92	6.76	6.11	6.05	5.67	5.86	6.21	6.09	6.18	6.50
2015	6.67	7.15	6.95	6.34	6.40	6.15	5.57	6.41	6.71	5.87	5.89	6.20
2016	6.46	6.98	7.15	6.51	6.27	5.54	5.33	6.32	6.62	5.78	6.05	6.22
2017	6.71	6.56	7.10	6.77	6.15	6.16	5.62	6.32	6.30	6.20	6.03	6.46
2018	6.58	6.75	6.87	6.11	5.88	5.22	5.25	5.80	6.48	5.77	5.97	6.04
2019	6.54	6.84	6.98	6.84	6.25	5.45	5.41	6.22	6.34	5.73	5.43	5.88
2020	6.15	6.87	6.31	6.39	6.67	6.20	5.42	5.67	6.19	6.21	6.18	6.14
Yearly average	6.52	6.94	6.95	6.52	6.28	5.75	5.37	6.17	6.41	5.96	5.99	6.22

Table 3.2: Yearly average of Monthly Irradiance, Temperature and Wind Speed for Boohe data 2011-2020 (Source: NASA) by Months

Month	Irradiance (KWh/m2/day)	Temperature ($^{\circ}C$)	Wind Speed (m/s2)
January	6.52	25.54	6.90
February	6.94	26.83	6.95
March	6.95	28.53	6.93
April	6.52	28.74	5.97
May	6.28	27.75	6.97
June	5.75	28.04	10.51
July	5.37	27.34	11.56
August	6.17	27.89	10.54
September	6.41	28.76	8.82
October	5.96	27.71	5.10
November	5.99	26.79	5.49
December	6.22	26.10	6.76
Average	**6.26**	**27.50**	**7.71**

The yearly average of monthly irradiance, temperature, and wind speed data for Boohe spanning from 2011 to 2020, sourced from NASA, Table 3.2, provides valuable insights into the climatic conditions of the region over the past decade. By aggregating monthly data, trends in solar radiation, temperature variations, and wind speeds visualized and analyzed comprehensively through graphical representations, Figure 3.5, 3.6, 3.4. These graphs illustrate seasonal patterns and also facilitate the identification of long-term trends and anomalies, aiding in the optimization of off-grid solar-diesel system design and energy management strategies tailored to Boohe's specific climatic characteristics.

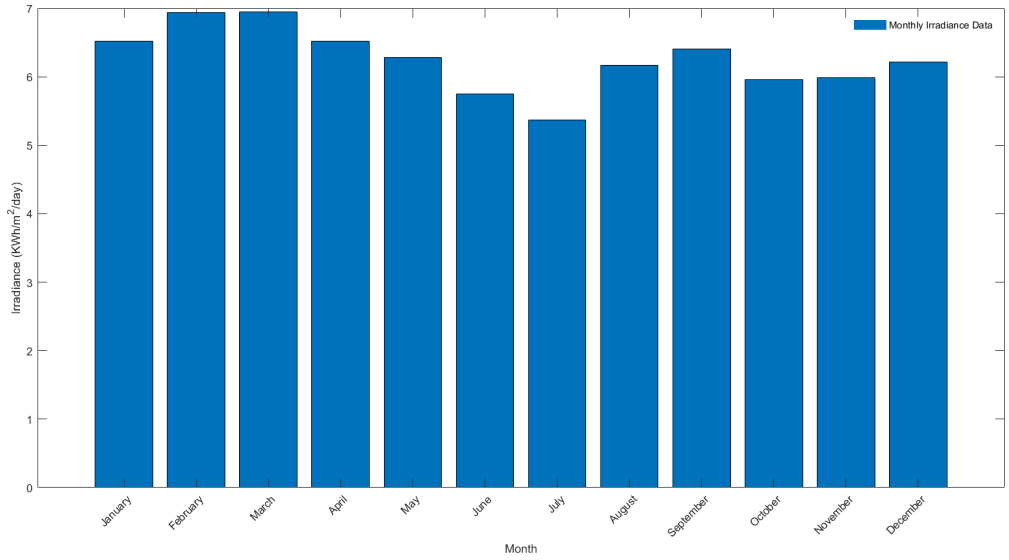

Figure 3.4: Monthly Irradiance data (NASA)

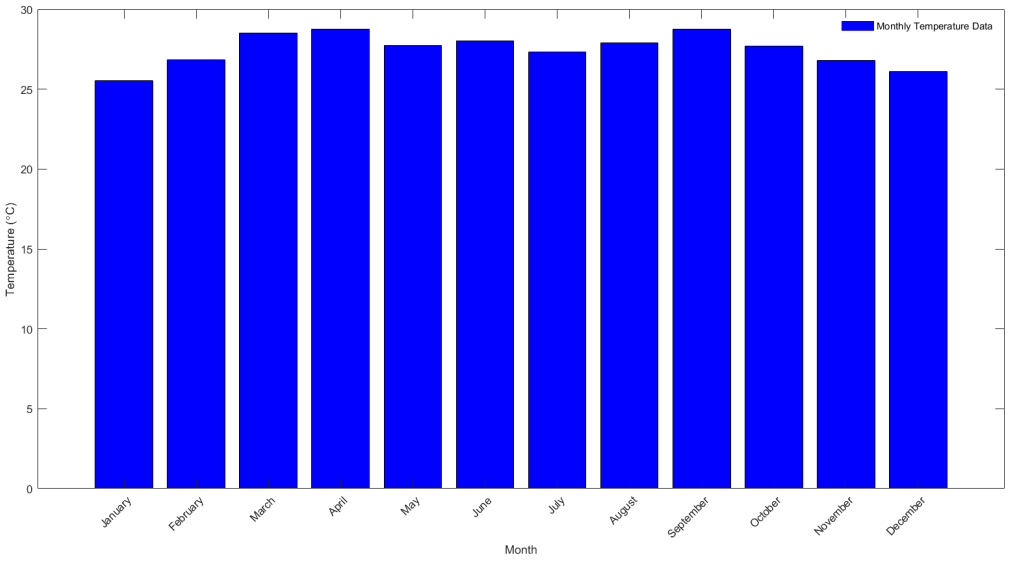

Figure 3.5: Monthly Temperature data (NASA)

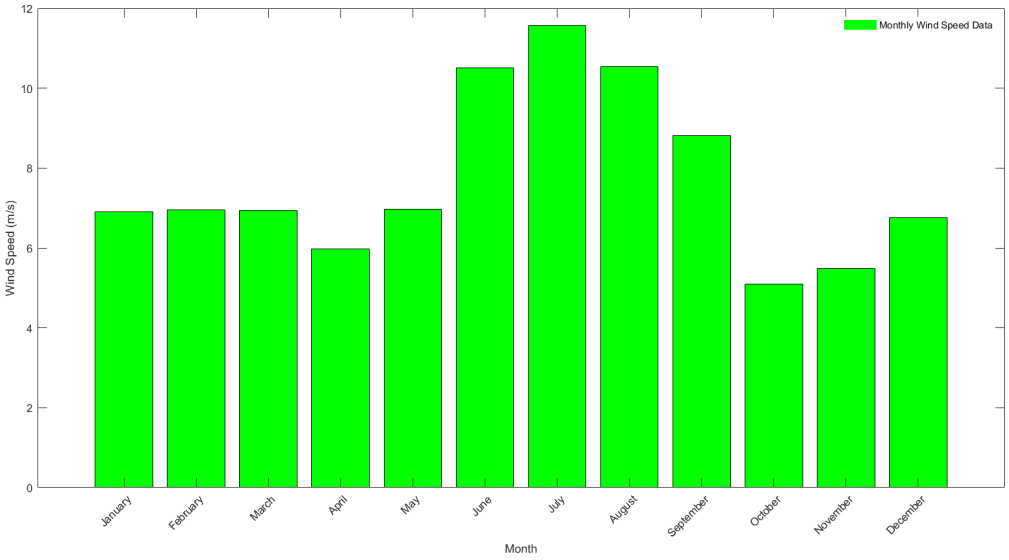

Figure 3.6: Monthly Wind Speed Data (NASA)

The irradiance data is available above given by tables and graphs. Hence, the subsequent phase involves the strategic selection of appliances for integration into the off-grid solar-diesel system. This selection process is crucial for ensuring that the system can adequately meet the energy demands of the intended applications while optimizing energy efficiency and resource utilization. To do so the most critical loads of the village are only included for power system load reduction to the over all system. Typically, this is identifying and prioritizing critical loads, which are those essential for maintaining key functionalities and services within the Boohe village. These critical loads are determined based on factors: safety, health, economic impact, and operational requirements of the society. By referencing this method the following appliance Table 3.3 is provided as a critical load on a daily basis of 24 hours time. From Table 3.3 data, a peak load of 54.65 kWh is recorded between 13:00 and 14:00, which corresponds to midday by Ethiopian local time. The total daily load requirement for the village is 399.21 kWh. This estimate includes contributions from residential households, commercial establishments, schools, hospitals, and other facilities. Although the specific breakdown is not detailed here, the summation of individual load profiles informed the total load requirement used for the system design.

Table 3.3: Daily Load Data by Time Interval

Time Interval	Domestic Load Estimation	Public Load Estimation	Commercial Load Estimation	Industrial Load Estimation	Total KWh
00:00-01:00	0.00	0.40	5.19	0.00	5.60
01:00-02:00	0.00	1.31	1.65	0.15	3.11
02:00-03:00	0.00	1.13	1.75	0.15	3.04
03:00-04:00	0.00	4.50	7.20	0.15	11.85
04:00-05:00	0.00	4.11	2.66	0.15	6.92
05:00-06:00	23.25	2.80	1.79	0.00	27.84
06:00-07:00	27.28	0.89	1.25	0.15	29.56
07:00-08:00	27.28	0.72	1.88	0.15	30.04
08:00-09:00	27.28	3.62	4.75	0.15	35.80
09:00-10:00	0.00	0.67	1.85	0.15	2.67
10:00-11:00	0.00	0.65	4.06	0.00	4.72
11:00-12:00	0.00	0.40	6.90	0.00	7.30
12:00-13:00	34.88	0.88	7.15	0.00	42.91
13:00-14:00	52.73	0.88	1.04	0.00	54.65
14:00-15:00	39.22	0.88	1.02	0.00	41.12
15:00-16:00	40.92	1.78	0.93	0.00	43.63
16:00-17:00	9.15	0.84	0.86	0.00	10.85
17:00-18:00	2.33	0.84	0.86	0.00	4.03
18:00-19:00	2.33	2.16	0.86	0.00	5.35
19:00-20:00	2.33	0.84	0.86	0.00	4.03
20:00-21:00	2.33	0.84	0.86	0.00	4.03
21:00-22:00	2.33	0.84	3.11	0.00	6.28
22:00-23:00	2.33	0.84	0.86	0.00	4.03
23:00-00:00	2.33	2.16	5.36	0.00	9.85
Total daily load	**298.25**	**35.02**	**64.74**	**1.21**	**399.21**

Table 3.3 presents daily load data categorized by time intervals, encompassing domestic, public, commercial, and industrial load estimations along with the total kilowatt-hour (kWh) consumption. Each time interval showcases the estimated energy demand for different sectors throughout a day. The plot of the total kWh data in graph of Figure 3.7 visualizes the fluctuation in energy consumption across the 24-hour period, highlights peak demand periods and trends in power usage patterns. The graphical representation helps to understand the distribution of energy consumption throughout the day.

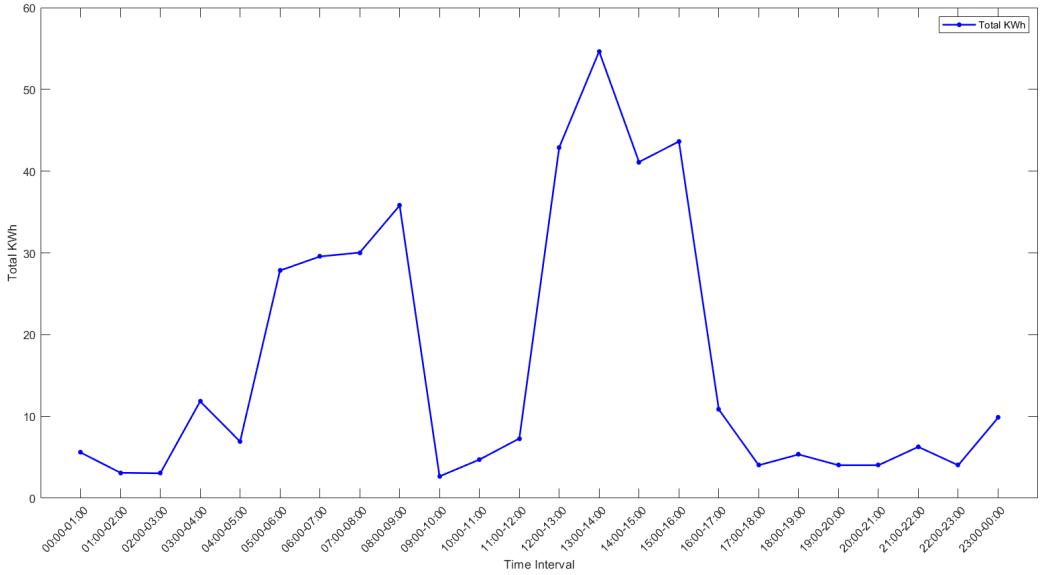

Figure 3.7: Daily Load Curve of Total KWh

3.2.2 Solar Power System Components

Solar photovoltaic system or solar power system is a renewable energy system which uses PV modules to convert directly sunlight into electricity. It has major components of: PV module, solar charge controller, inverter, battery bank, auxiliary energy sources i.e. diesel and appliances.

The PV module is a fundamental component of a solar photovoltaic (PV) system, playing a crucial role in converting sunlight into direct current (DC) electricity. The solar charge controller is essential for regulating the voltage and current from the PV panels to the battery, preventing overcharging and extending battery life [26]. The inverter converts the DC output of the PV panels into AC current suitable for powering appliances or feeding back into the grid. The battery bank stores excess energy generated by the system for later use when demand exceeds supply, ensuring a reliable power supply during periods of low solar irradiance. Auxiliary energy source is typically a diesel generator which supplement solar power generation during periods of failure to a PV system [27, 28]. Finally, the appliances connected to the system represent the load, utilizing the generated electricity for various purposes.

3.2.3 Solar PV System Sizing

Solar PV system sizing is a critical aspect of designing an efficient and effective solar power system [29]. It involves determining the appropriate capacity and configuration of PV modules, inverters, batteries, and auxiliary components to meet the energy needs of the intended application. The factors: the desired system output, location-specific solar irradiance levels, available space for installation, shading, orientation, and tilt angle of the PV panels, as well as the energy consumption patterns of the connected loads influence the sizing process [30]. By conducting a thorough analysis of these factors, the sizing of each component to ensure optimal performance, and reliability is discussed as follows.

3.2.3.1 Determine Power Consumption Demands

The first step in designing a solar PV system is to find out the total power and energy consumption of all loads that need to be supplied by the solar PV system. This is illustrated as follows:

1. Calculate total Watt-hours per day for each appliance used: Add the Watt-hours needed for all appliances together to get the total Watt-hours per day which must be delivered to the appliances [31, 32]. Hence, a total energy consumption of 399.21 kWh/day found from total daily load analysis is used for the following analysis.

$$\text{Annual energy consumption} = 399.21\text{kWh/day} * 365\text{day} = 145711.65\text{kWh} \tag{3.1}$$

$$\begin{aligned} \text{Average load demand per hour} &= \frac{\text{Annual energy consumption}}{8760\text{hr}} \\ &= \frac{145711.65\text{kWh}}{8760\text{hr}} \\ &= 16.6338\text{kW} \end{aligned} \tag{3.2}$$

Hence, the average load demand can be calculated as the total daily estimated load demand by twenty-four hours, i.e. 16.6338 kW.

The daily peak load of the system from the data table has a value of 54.65 kW. Hence the average load factor of the system is given by equation 3.3.

$$\text{Average load factor} = \frac{\text{Average load}}{\text{Peak load}} = \frac{16.6338\text{kW}}{54.65\text{kW}} = 30.4\% \tag{3.3}$$

In this thesis the whole load of the system is needed to-be supported with the PV system. The diesel and battery are required in case the PV couldn't support the whole system. Therefore, the PV system is designed to handle the worst case highest possible peak load of the system. The installed capacity of the system is given by equation 3.4, assuming a 10% loss. The selection of peak load approach prioritizes system reliability and avoids power shortages during critical times.

$$\begin{aligned} \text{Installed capacity} &= \text{Peak load} + \text{Loss} \\ &= 54.65\,\text{kW} + 5.465\,\text{kW} \\ &= 60.115\,\text{kW} \end{aligned} \tag{3.4}$$

Now lets select the appropriate PV system available from the market for the proceeding analysis as in table 3.4.

Table 3.4: JKM400M-72H Solar Panel Specification

Module type	JKM400M-72H
Maximum power (P_{max})	400W
Maximum power voltage (V_{mp})	41.7V
Maximum power current (I_{mp})	9.60A
Open circuit voltage (V_{oc})	49.8V
Short circuit current (I_{sc})	10.36A

Now the amount of PV modules needed for the required installed capacity above in equation 3.4 is determined for the PV panel using the data in table 3.4. The total power production from the solar PV modules given by equation 3.5.

$$\text{Solar PV output power} = \text{PV rated power} \times \text{Number of PV} \times \text{Converter efficiency} \tag{3.5}$$

Now the number of the solar panels (N_{PV}) is calculated using JKM400M-72H PV having 95% efficiency and rated power of 400W.

$$\begin{aligned} P_{PV} &= \text{PV rated power} \times N_{PV} \times \text{efficiency} \\ 60.115\text{kW} &= 400\text{W} \times N_{PV} \times 0.95 \end{aligned} \tag{3.6}$$

$$N_{PV} = 158.1974 \tag{3.7}$$

This number is rounded to the next integer number as a counting value of PV panel, i.e. 159 solar panels are required to support fully the daily load including the peak load of 54.65 kW.

2. Calculate the total load of the system for the panel connection design based on some desired preference system or bus voltage [33]. The bus voltage is often chosen based on the desired system voltage, which impacts the overall efficiency and performance of the PV system [34]. The system to-be designed here is needed to support a range of loads of: domestic, public, commercial, and industrial loads. The domestic and public loads usually need a bus voltage of 48 to 120V. However, a common bus voltage for many commercial and industrial PV systems is around 450V, therefore, a 450V system voltage will be designed accompanying all types of the listed loads. The system voltage is 450V then the load denoted with L in Ah is calculated by equation 3.8 as the division of total energy consumption to system voltage.

$$\begin{aligned} L &= \frac{\text{Daily energy demand}}{\text{Bus voltage}} \\ &= \frac{399.21\text{kWh/day}}{450\text{V}} \\ &= 887.1333\text{Ah/day} \end{aligned} \tag{3.8}$$

3.2.3.2 PV Modules Sizing

Different size of PV modules produce different amount of power. To find out the sizing of PV module, the total peak Watt produced need is needed. The peak Watt produced depends on size of the PV module and climate of site location. Panel generation factor is considered which is different in each site location. For Ethiopia, the panel generation factor is from 15% to 20%. The sizing of PV module presented as follows.

1. Calculate the total Watt-peak rating needed for PV modules: Multiply the total Watt-hours per day needed from the PV modules (L from above) by 1.3 to get the total Watt-peak rating needed for the PV panels needed to operate the appliances. i.e. The required power from solar array denoted with P_r is given by equation 3.9.

$$P_r = L * LF \tag{3.9}$$

Where L is load in Ah and LF is safety factor due to losses and dust on the module.

$$P_r = L * LF = 887.1333\text{Ah} * 1.3 = 1153.2733\text{Ah/day} \tag{3.10}$$

Power generated from module in Ah denoted by P_g and given by equation 3.11.

$$\begin{aligned} P_g &= \frac{P_{max}}{V_{mp}} * \text{antonomy} \\ &= \frac{400W}{41.7V} * 3\text{hr/day} \\ &= 28.78\text{Ah/day} \end{aligned} \tag{3.11}$$

2. Calculate the number of PV panels for the system: Divide the answer obtained in equation 3.10 by the results of equation 3.11. Any fractional part of the result is increased to the next highest full number and that will be the number of PV modules required.

   Result of the calculation is the minimum number of PV panels. If more PV modules are installed, the system will perform better and battery life will be improved. If fewer PV modules are used, the system may not work at all during cloudy periods

and battery life will be shortened. Hence, the total number of PV module is denoted with N is given by equation 3.12:

$$\begin{aligned} N &= \frac{P_r}{P_g} \\ &= \frac{1153.2733\text{Ah/day}}{28.78\text{Ah/day}} \\ &= 40.1 \approx 41 \end{aligned} \tag{3.12}$$

Number of PV in series denoted with N_{series} is given by equation 3.13, where the system voltage is considered tobe the maximum voltage of the boost converter tobe designed in the next chapter.

$$\begin{aligned} N_{series} &= \frac{\text{System voltage}}{\text{PV voltage}(V_{mp})} \\ &= \frac{\text{Bus voltage}}{V_{mp}} \\ &= \frac{300}{41.7} = 7.1949 \approx 8 \end{aligned} \tag{3.13}$$

To ensure system reliability and avoid power shortages during periods of highest demand, hybrid energy systems are typically designed to handle peak loads, especially for critical appliances. In the case of Bohe Village, the peak load demands 159 PV panels, while the average load only requires 41 panels. This discrepancy highlights the need to install more panels than the average calculation suggests, thereby ensuring the system can handle peak load and maintain continuous operation. This approach aligns with standard design practices in renewable energy systems, where systems are sized to meet peak demand to ensure stability and reliability. Studies such as those by Kumar and Sharma [35] and Singh and Prasad [36] emphasize the importance of designing hybrid systems with sufficient capacity to meet peak loads, thus ensuring optimal performance under varying conditions. Based on this premise, the number of PV panels in parallel, denoted by N_{parallel}, is

given by equation 3.14.

$$\begin{aligned} N_{parallel} &= \frac{N_{PV}}{N_{series}} \\ &= \frac{159}{8} = 19.875 \approx 20 \end{aligned} \tag{3.14}$$

Now the overall size of the PV panel is determined. The behavior of a solar panel described using the single-diode equivalent circuit model, which relates the output current I and voltage V to the solar irradiance G and temperature T. The equations 3.15, 3.16 governing this model are derived from Figure 3.8 below.

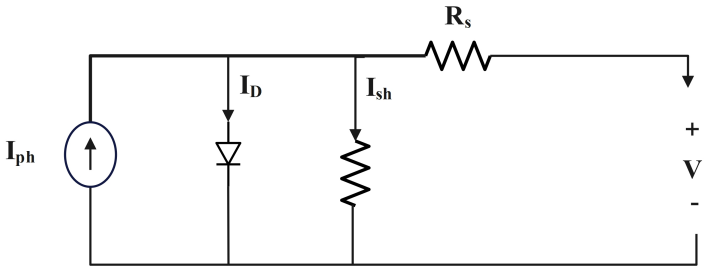

Figure 3.8: PV cell Equivalent Circuit

$$I = I_{\text{ph}} - I_{\text{s}} \left(e^{\frac{qV}{nkT}} - 1 \right) - \frac{V + IR_{\text{s}}}{R_{\text{sh}}} \tag{3.15}$$

$$P(V) = VI = V \left(I_{\text{ph}} - I_{\text{s}} \left(e^{\frac{qV}{nkT}} - 1 \right) - \frac{V + IR_{\text{s}}}{R_{\text{sh}}} \right) \tag{3.16}$$

where: I_{ph} is the photocurrent, I_{s} is the saturation current, q is the electron charge, k is the Boltzmann constant, n is the ideality factor, R_{s} is the series resistance, and R_{sh} is the shunt resistance.

MPPT algorithm aim to maximize the power output, $P(V)$ of the solar panel by dynamically adjusting the operating point V_{MPPT} based on the current environmental conditions. One common approach is the Maximum Power Point Tracking (MPPT) based Proportional Integral (PI) algorithm, which adjusts V_{MPPT} based on some required

error tolerance of the voltage.

$$V_{\text{MPPT}}(k+1) = \begin{cases} V(k) + \Delta V, & \text{if } \frac{dP}{dV} > 0 \\ V(k) - \Delta V, & \text{if } \frac{dP}{dV} < 0 \end{cases} \tag{3.17}$$

where ΔV is the perturbation step size.

3.2.4 Energy Storage Unit Selection and Sizing

In other types of power forms, electricity is more flexible in use because it is a highly organized form of energy that can be converted efficiently into other forms. But the demerit of electricity is that cannot be easily stored on a large scale. Almost all electric energy used today is consumed as it is generated. Photovoltaics are intermittent sources of power, and cannot meet the load demand at all times [17].

In this study, the electrochemical battery is chosen as the energy storage system, as it is widely used and well-known. The battery converts chemical energy into electrical energy, which can be used to stabilize and improve the power system's stability. Each cell in the battery contains a positive electrode, a negative electrode, and an electrolyte that isolates the electrodes. When the battery is connected to an electric circuit, a chemical reaction takes place in the electrolyte, causing ions to move [17]. This movement of electric charge creates an electric current that flows through the cell and the circuit it is connected. The main purpose of the battery in this study is to store electrical energy generated by the PV array. It will also smooth out any transients that may occur in the solar systems, providing a stable voltage and current level to electrical loads.

3.2.4.1 Battery Type Selection

There are two fundamental types of electrochemical batteries: primary and secondary batteries. Primary batteries are disposable batteries which are designed to be used once and discarded, while secondary batteries are rechargeable, in contrast to disposable ones, can be recharged and used multiple times, with a conversion efficiency ranging from 70% to 90% [34]. There are various types of rechargeable batteries, including Nickel Cadmium

(NiCd), Nickel Metal Hydride (NiMH), Lead Acid, and Lithium-ion (Li-ion) batteries. Presently, Lead Acid and Lithium-ion batteries are leading the market for rechargeable batteries. Although Lead Acid batteries are have lower cost and lower potential for overheating at high temperatures, Lithium-ion batteries are chosen for this study due to their offer over other rechargeable batteries.

Table 3.5: The Default Power Coefficient Constants

Parameters	**Lithium-ion**	**Lead acid**
Cost($)	5000-1500	500 - 1000
Nominal cell voltage(V)	3.6	2.0
Energy density(Wh/Kg)	150-250	30-40
Capacity(kWh)	15	1.5
Depth of discharge (%)	85	50
Efficiency (%)	90	80-85
Lifespan(years)	7-15	5-12

Hence, lithium-ion batteries are renowned for their high energy density, long lifespan, and superior efficiency, making them the preferred choice for a wide range of applications, from renewable energy storage to electric vehicles and portable electronics [37]. They offer a significant advantage in terms of weight and space savings due to their high energy density, allowing for more energy storage in a compact form. With an efficiency of around 90%, they ensure minimal energy loss during charging and discharging processes. Despite their higher initial cost, their longer lifespan (ranging from 7 to 15 years) and greater depth of discharge (up to 85%) make them a cost-effective and reliable option over time, offering both economic and performance benefits in the long run.

The battery type recommended for using in solar PV system is deep cycle battery. Deep cycle battery is specifically designed to-be discharged to low energy level and rapid recharged or cycle charged and discharged day after day for years [38]. The battery is required to-be large enough to store sufficient energy to operate the appliances at night and cloudy days or season of low light.

The Watt-hour (Wh) capacity of a fully charged battery that can power a load is determined by multiplying the voltage and ampere-hour values [39]. The state of charge indicates the amount of electric charge in relation to a full charge. When a battery is

connected in series with only its internal resistance, its no-load voltage is measured. The simplified electrical circuit of a battery's state is depicted below Figure 3.9 to illustrate how its internal impedance can be influenced by the charging level and temperature.

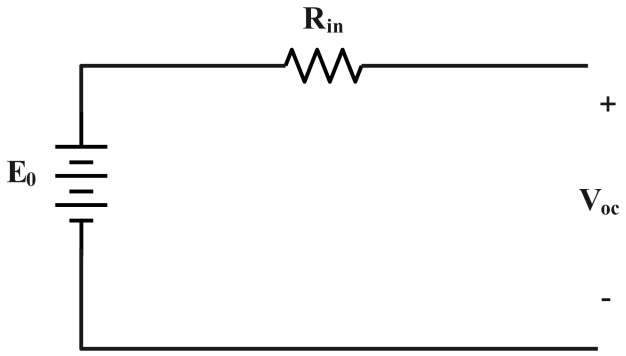

Figure 3.9: Simplified Electrical Circuit of a Battery

This simplified electrical circuit diagram of the battery is mathematically given by equation 3.18.

$$V_{oc} = E_0 - I_0 R_{in} \tag{3.18}$$

Where V_{oc}, I_0, and R_{in} are the battery open-circuit voltage, current, and internal resistance respectively and the open-circuit voltage is calculated using equation 3.19 [40].

$$E_0 = E_L - \frac{Q_{max}}{Q - \int_0^t f_b \cdot d\tau} + A^{-B\int_0^t f_b \cdot d\tau} \tag{3.19}$$

Where E_0, E_L, and Q are the battery constant voltage, the polarization voltage, and the battery capacity, f_b defines the actual battery charge, A is the amplitude of the exponential zone, and it is the inverse of the exponential zone time constant [41]. To avoid the depletion of the battery and prolong its life, its capacity must be maintained within the specified range at the state of charge. Hence, the battery state of charge (SOC) is mathematically expressed by the following equations.

$$SOC = 100\left(1 - \frac{1}{Q_{max}}\int_0^t f_b \cdot d\tau\right) \tag{3.20}$$

$$Q_{dis} = 0.5 \cdot Q_T^{0.5} \cdot Q_{sec}^{0.5} \tag{3.21}$$

Where Q_{dis} is the maximum capacity of the battery, Q_T is the nominal capacity of the battery, and Q_{sec} is the reserve discharge capacity of the battery. The charging process of the battery is not 100% efficient, just a portion of the absorbed energy reaches the storage, and the rest of the heat generated by the electrochemical reactions [42]. Thus, the state of charge (SOC) has been proposed in this work. Calculating the energy absorbed in the battery for each subsystem with battery hybrid type system typically involves tracking the number of ampere-hours absorbed, integrating the current and ampere-hours into the standby day calculated. The total switch state was marked based on the time, the day of operation was recommended critical as the number of days as an indicator and the total absorbed ampere-hour [43]. The load is not only over the day but based on the monthly load and the battery technical specification is recorded in Appendix A.

Calculating the number of batteries is mandatory for solar-diesel and battery hybrid power systems mainly depends on the average daily energy consumption, battery capacity, and days of autonomy which refers to the number of days a battery bank will supply a given load without being recharged by solar resource. For critical loads which must be used all the time, five days of autonomy are recommended even if the number of batteries and cost are increased simultaneously. If the load is not critical, one to three days of autonomy is commonly used [44]. Therefore, to find out the size of battery the following calculations are made.

1. Calculate total Watt-hours per day used by appliances.
2. Divide the total Watt-hours per day used by 0.85 for battery loss.
3. Divide the answer obtained in item 2 by 0.6 for depth of discharge.
4. Divide the answer obtained in item 3 by the nominal battery voltage.
5. Multiply the answer obtained in item 4 with days of autonomy (the number of days that you need the system to operate when there is no power produced by PV panels) to get the required Ampere-hour capacity of deep-cycle battery.

$$\text{Battery Capacity (Ah)} = \frac{\text{Total Wh per day used by appliances}}{0.85 * 0.6 * \text{nominal battery voltage}} * \text{days of autonomy} \tag{3.22}$$

The nominal battery voltage in solar-diesel mini-grid systems is typically chosen based on several factors: system's DC voltage compatibility, component compatibility, and the desired energy storage capacity. Common nominal voltages for batteries in such systems range from 12V to 450V per battery bank. Here in this thesis the 450V nominal battery voltage is selected. The total battery capacity and number of batteries are calculated in the following equations. The average demand of the system was calculated earlier, 16.6338 kW. The total Ah for the battery design is calculated as follows equation 3.23.

$$\text{Battery Capacity (Ah)} = B_c = \frac{399.21 \text{ kWh}}{0.85 * 0.6 * 450\text{V}} * 1 = 1739.4771\text{Ah} \tag{3.23}$$

The storage battery selected for this thesis is Lithium-ion battery with the specifications:voltage: 450V, capacity: 5Ah, and energy capacity: $450V \times 5Ah = 2250Wh$. Now the number of storage batteries are calculated by equation 3.24.

$$\text{Number of Batteries in Parallel} = B_{bp} = \frac{\text{Usable Energy Storage Required in Wh}}{\text{Energy capacity of one battery in Wh}} \tag{3.24}$$

$$B_{bp} = \frac{B_c}{B_{nc}} = \frac{782764.706}{2250} = 347.8956 \approx 348 \tag{3.25}$$

The series connected batteries are found using equation 3.26.

$$B_{bs} = \frac{\text{Bus voltage}}{\text{Nominal voltage}} = \frac{450}{450} = 1 \tag{3.26}$$

The total number of batteries (N_b) which is required for the system is the product of series and parallel connected batteries, 348. To ensure the battery system can handle the

peak load, let's calculate the current during peak load 3.27.

$$\begin{aligned} \text{Peak Load Current} &= \frac{54.65 \text{ kW}}{450 \text{ V}} \approx 121.4444 \text{ A} \\ \text{Battery String Current} &= 5 \text{ Ah} \times 348 \approx 1740 \text{ Ah} \end{aligned} \tag{3.27}$$

This means that a single string can easily handle the peak load current, and thus the battery bank of 348 parallel strings each with one battery in series will be sufficient.

3.2.5 Inverter Sizing

The system to be designed in this thesis is going to be providing an AC load of appliance. Hence, an inverter is used in the system where AC power output is needed. The input rating of the inverter is selected not to-be lower than the total watt of appliances. The inverter nominal voltage is selected to-e the same as the nominal battery voltage [45]. For stand-alone systems, the inverter must be large enough to handle the total amount of Watts used at one time. The inverter size should be 25-30% bigger than total Watts of appliances [46, 47]. In case of appliance type is motor or compressor then inverter size should be minimum 3 times the capacity of those appliances and must be added to the inverter capacity to handle surge current during starting.

In inverter sizing for off-grid systems, the input rating of the inverter should be appropriately matched to the capacity of the PV array to ensure safe and efficient operation. Off-grid systems typically do not rely on a direct connection to the grid, meaning the inverter must independently handle fluctuations in energy demand and supply. Generally, residential off-grid systems use 230V/50 Hz single-phase connections for battery charging and energy storage. Inverter sizing calculations are performed using the available load profile and energy requirements of the off-grid system. The sizing is typically based on factors such as peak demand, battery capacity, and operational constraints to ensure reliable and continuous power supply.

The first phase is the identification of the maximum (peak) load, and from table 3.3,

the maximum hourly load is given by equation 3.28.

$$\text{Maximum hourly load} = 54.65 \text{ kW (13:00-14:00)} \tag{3.28}$$

The second phase is the calculation of the required inverter capacity, hence considering an inverter efficiency of 97% it will be calculated as in equation 3.29.

$$\text{Inverter capacity (efficiency adjusted)} = \frac{\text{Maximum hourly load}}{\text{Inverter efficiency}} = \frac{54.65 \text{ kW}}{0.97} \approx 56.34 \text{ kW} \tag{3.29}$$

The last phase is the consideration of the safety margin, and it's assumed that a safety margin of 15% enough for this system.

$$\text{Final inverter capacity} = 56.34 \text{ kW} \times 1.15 \approx 64.79 \text{ kW} \tag{3.30}$$

3.3 Diesel System Design

The case study in this thesis research encompasses a load of about 399.21kWh/day. In the design of this load mini grid system, the diesel generator plays a critical role in ensuring a reliable power supply, particularly during periods of low solar generation and high energy demand. The diesel system design encompasses several key components and considerations to optimize performance and efficiency [18].

The diesel generator is sized based on the peak load demand and the total energy requirements of the mini grid [48]. The generator must be capable of supplying sufficient power to meet the maximum load at any given time. In most literature's a typical generator with a capacity of 100kW to 200kW is considered, depending on the load profile and the expected duration of peak demand periods [49]. In this thesis the diesel generator is required to operate for 4 hours supporting all the load in a stand alone operation. Hence, there is 54.56 kWh peak load load for the generator to operate functionally a 100kW power rating is enough supplying the all the appliance about 4 hours.

Let's start with identification of the peak load and energy demand from the given load profile table 3.3 i.e. peak load of 54.65 kWh (from 13:00-14:00), and total daily energy

demand of 399.21 kWh. Assuming a 30% margin on the peak load the diesel generator capacity is selected based on equation 3.31.

$$\text{Required Capacity} = 54.65 \text{ kWh} \times 1.3 \approx 71 \text{ kW} \tag{3.31}$$

Hence, the generator with a capacity slightly higher than this value is selected, a 100 kW generator. Assuming the generator runs for 4 hours per day to meet the peak load periods, has efficiency of 30% and a fuel consumption rate of 0.24 liters per kWh then the energy supplied by the generator running for 4 hours at full capacity given by 3.32.

$$\text{Energy Supplied by Generator} = 100 \text{ kW} \times 4 \text{ hours} = 400 \text{ kWh} \tag{3.32}$$

The fuel consumption for this running generator is finally calculated by equation 3.33.

$$\text{Fuel Consumption} = 400 \text{ kWh} \times 0.24 \text{ liters/kWh} = 96 \text{ liters/day} \tag{3.33}$$

For the practical scenario the maintenance and operational considerations are critical in the diesel system design. Regular maintenance schedules needed to-be established to ensure the reliability and longevity of the generator: routine checks of the engine, fuel system, cooling system, and electrical connections. Efficient fuel management practices: fuel quality monitoring and proper storage, are essential to prevent contamination and degradation. However, in this thesis the simulation scenario is considered and the permanent magnet synchronous machine will be used substituting the diesel generator.

3.4 Hybrid System Design

Hybrid system design encompasses the overall configuration and physical layout of the mini grid energy system. This is about determining the appropriate sizing and placement of components; solar panels, diesel generators, batteries, inverters, and related infrastructure [50]. Design considerations revolve around matching the capacities of these components with the expected load requirements and operational conditions [51]. The goal is

to design a system which integrates all the systems listed earlier and produce a working hybrid model in MATLAB Simulink. Factors: peak load demand, solar irradiance levels, and fuel availability dictated the design choices, ensuring that the hybrid system can reliably meet the energy needs of the mini-grid.

The integration of the all the components of the mini grid is managed by the hybrid controller, energy management system (EMS) [52]. To enhance the efficiency of each subsystem, advanced control strategies are implemented.

Chapter 4

System Optimization and Optimal Control Design of Hybrid System

Exploration of renewable energy sources is driven by the potential future scarcity of conventional resources. Renewable energy resources have significant drawbacks, including dependency on geographical locations and environmental conditions. High initial costs, increased maintenance expenses, and varying depreciation rates also present challenges for these hybrid systems [53]. The unpredictable nature of natural resources necessitates the development of hybrid systems capable of generating the maximum possible energy for continuous and reliable operation. Factors such as site conditions, energy availability, source efficiency, and technical and social limitations influence hybrid system design. In this context, employing an optimal sizing method is crucial to achieve high reliability and quality at the lowest cost. Key components of hybrid energy systems include renewable power sources, nonrenewable generators, control units, storage systems, and loads or grids, which may sometimes be AC/DC [54], however the AC loads are considered here in this research.

The Figure 4.1 provided illustrates a hybrid energy system comprising several interconnected components designed to ensure efficient and reliable energy management. The detailed explanation of each component and their interactions within the system is given below underneath the figure.

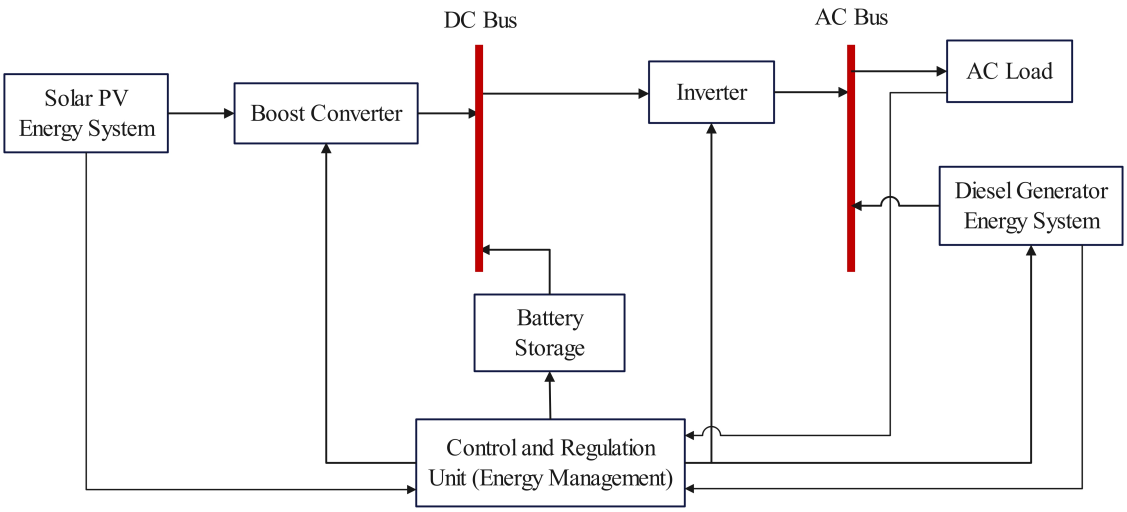

Figure 4.1: Solar Photovoltaic and Diesel based Hybrid Energy System

The solar PV energy system is a key component of the hybrid energy setup. It harnesses solar energy and converts it into electrical power through photovoltaic cells. This system is environmentally friendly, as it utilizes a renewable energy source [15]. Solar PV systems are particularly beneficial in areas with abundant sunlight, contributing significantly to the overall energy mix [3, 9]. The generated electricity from the Solar PV system is directed towards the control and regulation unit for further management.

The diesel generator energy system acts as a complementary power source within the hybrid setup. It provides a reliable backup power solution, particularly during periods when solar energy is insufficient due to weather conditions or nighttime [20, 21]. Diesel generators are known for their robustness and ability to generate a steady power output [18, 48]. In this system, the diesel generator feeds electricity into the control and regulation unit, ensuring that there is a continuous supply of power regardless of solar energy availability [49, 52].

The control and regulation unit is the central hub of the hybrid energy system, responsible for managing and optimizing the flow of energy from various sources [55, 56]. This unit plays a critical role in balancing the energy input from both the solar PV and diesel generator systems. It regulates the distribution of power to different components

and ensures that the energy demands of the load are met efficiently [57]. Furthermore, it manages the charging and discharging cycles of the battery storage system, optimizing energy use and storage.

Battery storage is an essential component for storing excess energy generated by the solar PV system. During periods of high solar energy production, any surplus electricity is stored in the batteries [32]. This stored energy can then be utilized when solar generation is low or during peak demand times, ensuring a consistent power supply [37]. The Battery storage system enhances the reliability and stability of the hybrid energy system by providing a buffer against energy fluctuations and outages [41, 44].

The inverter is a crucial device within the hybrid system that converts direct current (DC) electricity generated by the solar PV system and stored in the batteries into alternating current (AC) electricity, which is suitable for use by most household appliances and industrial equipment [45, 46, 47]. The inverter ensures that the power output is compatible with the load requirements. It also plays a role in synchronizing the energy from different sources to provide a seamless power supply to the load.

The load represents the end-users of the generated electricity, which include residential, commercial, and industrial consumers [58]. The hybrid energy system aims to supply a reliable and consistent flow of electricity to meet the demands of the load. The control and regulation unit ensures that the load receives power from the most efficient and available source, whether it be directly from the solar PV system, diesel generator, or the battery storage.

Finally, the integration of these components within the hybrid energy system maximizes efficiency and reliability. The system intelligently switches between solar, battery banks, and diesel power based on availability and demand, ensuring an uninterrupted power supply. The use of battery storage allows for energy savings and improved load management, reducing reliance on diesel generators and minimizing fuel consumption. The control and regulation unit's role in optimizing energy flow and storage enhances overall system performance, leading to cost savings and environmental benefits. The typical controls are: boost controller, battery charging, inverter, and energy management system.

4.1 Maximum Power Point Tracking (MPPT) Controller Design for Boost Converter

In this section, the design of a Maximum Power Point Tracking (MPPT) controller for a boost converter in a photovoltaic (PV) system is presented. The objective is to adjust the duty cycle of the boost converter to maintain the PV panel's operating voltage between 200V and 300V, with the grid system operating at 500V. The duty cycle D of the boost converter is designed to be varying between values of 0.4 and 0.6.

A boost converter is a DC-DC converter used to step up the input voltage V_{in} of the PV panel to a higher output voltage V_{out}. The relationship between the input voltage, output voltage, and the duty cycle D in the boost converter is given by equation 4.1.

$$V_{out} = \frac{V_{in}}{1 - D} \tag{4.1}$$

where $0 < D < 1$ is the duty cycle. For the PV system, V_{in} represents the voltage generated by the PV panel, and V_{out} is the voltage at the output of the boost converter.

The power P_{pv} generated by the PV panel is given by equation 4.2.

$$P_{pv} = V_{pv} \times I_{pv} \tag{4.2}$$

where V_{pv} and I_{pv} are the voltage and current of the PV panel, respectively.

The goal of the MPPT controller is to adjust the duty cycle D to ensure that the PV panel operates at its maximum power point (MPP). The MPP is characterized by the condition in equation 4.3, where there is no variation at the maximum power.

$$\frac{dP_{pv}}{dV_{pv}} = 0 \tag{4.3}$$

4.1.1 Perturb and Observe (P&O) Algorithm

The Perturb and Observe (P&O) algorithm is one of the most commonly used methods for Maximum Power Point Tracking (MPPT) in photovoltaic (PV) systems [17]. This

technique operates on a straightforward principle: it periodically perturbs the operating voltage of the PV panel and observes the resulting change in power output. The goal is to find the maximum power point (MPP) where the PV system operates most efficiently [40]. By increasing or decreasing the voltage slightly, the algorithm monitors whether the power output has increased or decreased. If the power increases, the perturbation continues in the same direction. Conversely, if the power decreases, the direction of the perturbation is reversed. This process ensures that the system converges towards the MPP.

One of the primary advantages of the P&O algorithm is its simplicity and ease of implementation, hence there is a desire to see practical applications of the renewable energy system in Ethiopia by this period [55]. However, it has some limitations, particularly under rapidly changing environmental conditions like fluctuations in solar irradiance or temperature. In such cases, the algorithm might fail to track the true MPP accurately, as it could oscillate around the point or track in the wrong direction. Despite these challenges, the P&O method remains widely adopted due to its balance between performance and computational simplicity, making it suitable for real-time applications in PV systems. The algorithm works as follows:

1. Measure the current voltage $V_{pv}(k)$ and current $I_{pv}(k)$.
2. Calculate the current power $P_{pv}(k) = V_{pv}(k) \times I_{pv}(k)$.
3. Compare the current power $P_{pv}(k)$ with the previous power $P_{pv}(k-1)$.
4. Adjust the duty cycle D based on the comparison:
   - If $P_{pv}(k) > P_{pv}(k-1)$, increase or decrease D depending on whether $V_{pv}(k)$ increased or decreased.
   - If $P_{pv}(k) < P_{pv}(k-1)$, reverse the direction of D adjustment.
5. Repeat the process.

The duty cycle D is constrained within the range $0.4 \leq D \leq 0.6$ to ensure that the PV panel voltage remains between 200V and 300V. The MPPT controller is implemented

using a digital control system. The control algorithm adjusts the pulse width modulation (PWM) signal that controls the switching of the boost converter's transistor. The input output mapping relationship is given by equation 4.1.

In this thesis the system is grid-connected where the grid voltage is 500V, the boost converter steps up the PV panel voltage V_{pv} to match the grid voltage. The MPPT controller ensures that the PV panel operates at the maximum power point by adjusting the duty cycle within the specified range.

4.2 Proportional-Integral (PI) Battery Charging Controller Design

The Proportional-Integral (PI) controller is commonly used in battery charging systems to maintain optimal charging conditions. The PI controller adjusts the charging current based on the difference between the desired and actual battery state of charge (SOC). The key advantage of using a PI controller is its ability to reduce the steady-state error, improve the overall system stability, and less cost and simplicity for practical applicability of the control method. The design of the PI controller needs to be aligned with the charge control method used in the system. In PV systems, the most common charge control methods are Pulse Width Modulation (PWM) and Maximum Power Point Tracking (MPPT), each method has its own implications for the design of the PI controller [55].

PWM controllers adjust the charging current by varying the duty cycle of the pulse signal. The PI controller in PWM systems is tuned to manage this duty cycle effectively, ensuring the battery receives the correct amount of charge while minimizing the ripple and maximizing the efficiency of the charging process [56].

MPPT controllers optimize the power output from the solar panels by adjusting the operating point to the maximum power point. The PI controller in an MPPT system is responsible for regulating the output voltage or current based on the MPPT algorithm's recommendations. This involves adjusting the duty cycle of the converter to match the optimal charging conditions [57]. The effectiveness of the PI controller is influenced

by the chosen MPPT technique. Classical MPPT techniques require different PI tuning compared to more advanced hybrid methods, hence, the application of Bacterial Foraging Algorithm (BFA) is utilized in this thesis research. The PI controller's parameters need tobe adjusted to handle the dynamic changes in power output and maintain optimal battery charging.

The solar charge controller is typically rated against ampere and voltage capacities of the system. The solar charge controller is selected accordingly to match the voltage of PV array and batteries. The solar charge controller should to has enough capacity to handle the current rating from the PV array. Hence, the sizing of controller depends on the total PV input current which is delivered to the controller and also depends on PV panel configuration (series or parallel configuration). According to standard practice, the sizing of solar charge controller is generally given by equation 4.4.

$$\text{Solar charge controller rating} = \text{Total short circuit current of PV array} * 1.25 \quad (4.4)$$

Both MPPT and PWM can monitor battery temperature to prevent overheating and modify the charging rates based on the energy storage charge level to enable charging closer to the battery's maximum capacity [55]. These methods have different capabilities in-terms of their application area and specification, presented at Table 4.1.

Table 4.1: The default power coefficient constants [55]

Conditions	**PWM**	**MPPT**
Voltage	PV array, and battery voltages should match	PV array voltage will be higher than the battery voltage
Battery voltage	Works at battery voltage	Works above battery voltage
System size	Applicable in lower power systems.	150 -200W or higher
Grid-Tie or Standalone	Used for standalone PV modules with Vmax 17 to 18V for 12V nominal battery voltage	Used for lower-cost standalone or grid-tie PV Modules
Sizing	PV array and WT sized in amps	PV array and WT sized in watts

Referring to Table 4.1, MPPT is preferred over PWM for this thesis research. The efficiency of photovoltaic systems is influenced by sunlight, and MPPT optimizes energy capture by adjusting system parameters to the changing sunlight. It keeps the PV panel at the Maximum Power Point (MPP) for maximum power generation [57].

MPPT, an active tracking system, uses electronic components to adjust the PV panel's orientation, maximizing energy capture. Unlike passive systems, which rely on mechanical movements and are less efficient, MPPT directly controls the system's output, making it a more cost-effective and efficient solution for solar energy optimization in this thesis.

Table 4.2: The Different MPPT Techniques

Classical	**Intelligent**	**Optimization**	**Hybrid**
Constant voltage	Fuzzy Logic Control (FLC)	Particle Swarm Optimization (PSO)	FLC-P&O
Hill climbing	Artificial Neural Networks (ANN)	Anti-Colony Optimization (ACO)	PSO-P&O
Perturb and Observe	Sliding Mode Control (SMC)	Grey wolf optimization (GWO)	ACO-P&O
Incremental Conductance	Support Vector Machines (SVM)	Bacterial Foraging Algorithm (BFA)	BFA-P&O
Fractional Short Circuit	Deep Learning (DL)	Genetic Algorithm (GA)	FLC-PSO
Fractional Short Circuit	Reinforcement Learning (RL)	Whale Optimization Algorithm (WOA)	ANFIS

The classical MPPT technique is commonly used by different authors due to the simplicity of algorithms, robustness, easier of implementation, and faster response, but it only considers uniform irradiation condition as the PV will generate one Global Maximum Power Point (GMPP) tracking and have rapid oscillations around MPP which is subjected to a loss of power. The difficulty of precisely tracking the GMPP out of multiple local MPPs (LMMP) isn't well accomplished by intelligence or optimization techniques independently [56, 57]. However, in this thesis the case study (Boohe) has largely uniform irradiation data very close to the average profile. Hence, the hybrid MPPT technique is formulated by combining the classical PI, and Bacterial Foraging Algorithm (BFA) optimization technique to obtain a better performance.

PI control is an effective strategy for managing battery charging in hybrid energy systems. It offers simplicity and robustness in maintaining the battery's State of Charge (SOC) within a desired range, ensuring efficient charging and prolonging battery life. The overall battery model with SOC dynamics was discussed in chapter 3 of section 3.2.4.1.

The control objective is to maintain the battery SOC within a desired range, ensuring efficient charging. Let the desired SOC be SOC_{ref}. The control error $e(t)$ is defined as the difference between the desired SOC and the actual SOC, as given by equation 4.5.

$$e(t) = SOC_{ref} - SOC \tag{4.5}$$

The dynamics of the SOC from equation 3.20 can be expressed in terms of the battery current I_b as follows:

$$\dot{SOC} = -\frac{I_b}{Q_{max}} \tag{4.6}$$

The PI controller adjusts the battery charging current I_b based on the error $e(t)$ and its integral over time. The PI control law is given by equation 4.7.

$$I_b(t) = k_p \cdot e(t) + k_i \cdot \int_0^t e(\tau)\, d\tau \tag{4.7}$$

where k_p is the proportional gain and k_i is the integral gain. The proportional term $k_p \cdot e(t)$ responds to the current error, while the integral term $k_i \cdot \int_0^t e(\tau)\, d\tau$ accumulates past errors to eliminate steady-state error.

The PI controller tuned with the BFA to ensure that the charging current I_b maintains the SOC close to SOC_{ref} while avoiding overcharging or excessive current. The tuning of k_p and k_i is crucial for achieving the desired performance and stability in the battery charging process. The control input $I_b(t)$ is designed to respect the battery's charging limits and avoid overcharging. This ensures that the charging process is both efficient and safe for the battery's longevity.

4.3 Inverter Control System Design

Proportional-Integral control is a widely used technique for regulating the operation of inverters in hybrid solar-diesel mini grid systems. This control strategy optimizes the utilization of solar energy by converting DC power from solar panels into AC power synchronized with the grid for load requirements [45, 46, 47].

The primary objective of using a PI controller in inverter control is to achieve efficient Maximum Power Point Tracking (MPPT) of the solar panels. The MPPT point V_{MPPT} varies with environmental conditions such as solar irradiance and temperature, affecting the voltage V of the solar panel. The PI control strategy aims to minimize the error between the reference MPPT voltage and the actual solar panel voltage.

The control error $e(t)$ is defined as in equation 4.8.

$$e(t) = V_{\text{MPPT}} - V \tag{4.8}$$

where V_{MPPT} is the reference voltage and V is the actual voltage of the solar panel.

The PI control law adjusts the control input $u(t)$ based on this error $e(t)$ and its integral over time. The PI control law is given by equation 4.9.

$$u(t) = k_p \cdot e(t) + k_i \cdot \int_0^t e(\tau)\, d\tau \tag{4.9}$$

where k_p is the proportional gain and k_i is the integral gain. The proportional term $k_p \cdot e(t)$ responds to the current error, while the integral term $k_i \cdot \int_0^t e(\tau)\, d\tau$ accumulates past errors to eliminate steady-state error.

The PI controller adjusts the duty cycle of the inverter to match the MPPT voltage V_{MPPT}. By dynamically tuning the control input $u(t)$ based on the error between the desired and actual voltage, the PI controller maintains optimal operation of the inverter, ensuring efficient power conversion from the solar panels.

The effectiveness of the PI controller lies in its ability to continuously adjust the inverter operation to track the MPPT point V_{MPPT} despite fluctuations in solar conditions. Proper tuning of k_p and k_i through BFA ensures that the inverter maintains optimal

performance, maximizing the power output from the solar panels while minimizing deviations from the MPPT voltage.

4.4 Energy Management System Controller Design

The Energy Management System (EMS) is a critical component of the hybrid energy system, responsible for managing power flows among the photovoltaic (PV) system, battery storage, and a diesel generator (DG). The EMS ensures efficient utilization of energy resources, optimal operation of the system, and reliable supply to meet demand under varying conditions of solar irradiance, battery state of charge (SOC), and load demand.

4.4.1 EMS Algorithm Description

The EMS algorithm dynamically determines power allocation based on the following input variables:

- Average PV power (P_{pvAvg}): The mean power generated by the PV system.
- Power demand (P_{dem}): The load demand of the system.
- State of charge (SOC): The current charge level of the battery.

The algorithm operates according to the following logic:

1. **Threshold Parameters:** The EMS considers key parameters, including:
    - Critical load (P_{ldCrt}): The minimum load that must always be supplied.
    - Maximum charge power (P_{chrgMax}) and maximum discharge power (P_{dchrgMax}): Constraints on battery charging and discharging rates.
    - Maximum and minimum SOC (SOC_{max} and SOC_{min}): Limits to protect battery health.
2. **Surplus PV Power:** When $P_{\text{pvAvg}} > P_{\text{ldCrt}} + P_{\text{dem}}$, the EMS calculates the surplus power (P_{net}).

- The diesel generator (P_{DG}) is turned off.
- If the SOC is below SOC_{max}, the surplus power is used to charge the battery, up to P_{chrgMax}.
- If the SOC reaches SOC_{max}, no further charging occurs.

3. **Deficit PV Power:** When $P_{\text{pvAvg}} \leq P_{\text{ldCrt}} + P_{\text{dem}}$, the EMS calculates the power deficit (P_{net}).
   - If the SOC is above SOC_{min}, the battery discharges to supplement the deficit, within the limit of P_{dchrgMax}.
   - Any remaining deficit is supplied by the diesel generator (P_{DG}).
   - If the SOC is below SOC_{min}, the diesel generator fully compensates for the deficit.

4.4.2 EMS Algorithm in Pseudocode

The EMS algorithm expressed in pseudocode as:

```
Inputs: P_pvAvg, P_dem, SOC
Constants: P_ldCrt, P_chrgMax, P_dchrgMax, SOC_max, SOC_min

If P_pvAvg > P_ldCrt + P_dem:
P_DG = 0
P_net = P_pvAvg - P_ldCrt - P_dem
If SOC < SOC_max:
P_chrg = min(P_net, P_chrgMax)
Else:
P_chrg = 0
Else:
P_net = P_pvAvg - P_ldCrt - P_dem
If SOC > SOC_min:
P_chrg = -min(abs(P_net), P_dchrgMax)
```

```
If abs(P_net) > P_dchrgMax:
P_DG = abs(P_net) - P_dchrgMax
Else:
P_DG = 0
Else:
P_chrg = 0
P_DG = abs(P_net)

Output: P_bat = P_chrg, P_DG, P_net
```

This EMS algorithm prioritizes the use of renewable energy from the PV system. Battery storage manages energy surpluses and deficits while adhering to SOC limits to ensure longevity. The diesel generator is employed only when renewable resources and battery power are insufficient to meet demand. This hierarchical approach optimizes the system's efficiency and minimizes reliance on non-renewable resources.

4.5 Optimization of Energy Management System Using Bacterial Foraging Optimization Algorithm (BFOA)

The optimization process of the Energy Management System (EMS) for a hybrid energy system is carried out using an improved Bacterial Foraging Optimization Algorithm (BFOA). The EMS is responsible for managing the distribution of power between key system components, including the photovoltaic (PV) system, battery storage, and Voltage Source Converter (VSC), ensuring efficient power usage under varying conditions. In addition to optimizing power distribution, the BFOA is employed to fine-tune the parameters of the PI controllers associated with the system. This dual function—both optimizing the control parameters and managing the power flow—ensures the hybrid system performs optimally. The cost function, derived from system performance in a Simulink model, is minimized to enhance overall system efficiency.

4.5.1 Bacterial Foraging Optimization Algorithm (BFOA)

The BFOA is inspired by the foraging behavior of *Escherichia coli* bacteria and is designed to solve complex optimization problems by simulating the chemotaxis, reproduction, and elimination-dispersal behavior of bacteria. The optimization process involves a population of bacteria, each representing a potential solution, which moves through the search space in a process called chemotaxis, adjusting its position based on the cost associated with that position [4, 55].

The integration of BFOA with PI for MPPT offers advantages such as robustness against varying environmental conditions and efficient tracking of the MPP. However, the following challenges are considered through this method: parameter tuning, computational complexity, and ensuring real-time implementation feasibility. Therefore, the BFO is employed to optimize the gain parameters of parameters the designed battery, boost, and inverter controllers.

In this implementation, the BFOA optimizes six parameters corresponding to the proportional and integral gains of the battery control system's PI controller, as well as the PV boost controller and the inverter controller gains. The BFOA has the following main steps.

- **Chemotaxis:** Bacteria move in random directions and update their positions based on the cost function. The cost function calculates the mean squared error (MSE) of key system variables such as battery current, dq currents, and DC voltage from the Simulink model. Bacteria with better positions (lower cost) continue to move in the same direction (swim), while others change direction (tumble).

- **Reproduction:** After a specified number of chemotactic steps, the least fit bacteria are eliminated, and the fitter bacteria replicate, ensuring that the population size remains constant.

- **Elimination and Dispersal:** To avoid local minima and maintain diversity in the population, a certain percentage of bacteria are randomly dispersed to new positions after a fixed number of reproduction steps.

4.5.2 Simulation Setup and Cost Function

The Simulink model used for the optimization developed incorporating all the necessary blocks, with the lower and upper bounds of the controller parameters defined in MATLAB functions. The cost function is defined to measure the system's performance by combining the MSE values of the battery current, dq currents, and DC voltage, providing a single metric to be minimized during optimization.

The cost function is designed to evaluate the performance of the system by combining the Mean Squared Error (MSE) values of three key components: the battery current, dq currents, and DC voltage. Each of these components is critical to the operation of the hybrid energy system, and their respective MSEs reflect how well the system is performing in terms of stability and efficiency. By combining these MSE values into a single cost metric, the function provides a unified measure of the system's overall performance. During the optimization process, this cost function is minimized to achieve the best controller parameter set, guiding the system toward optimal performance.

In this context, the Bacterial Foraging Optimization Algorithm (BFOA) is employed to iteratively optimize the controller gains. The parameters of the algorithm include a population of 20 bacteria, 5 chemotactic steps, 8 swims per chemotactic step, 5 reproduction steps, and 5 elimination-dispersal events with a dispersal probability of 0.2. The chemotactic step size is set to 0.05. Through these iterations, the algorithm seeks to minimize the cost function by adjusting the controller parameters, ultimately identifying the optimal set of gains. Upon successful completion of the optimization process, the BFOA delivers the optimal controller gain values, leading to enhanced performance in managing the hybrid energy system's efficiency and stability.

4.5.2.1 Cost Function Analysis

The cost function is defined to evaluate how well the system performs by combining the Mean Square Error (MSE) values of three important components: battery current, dq currents of inverter, and DC voltage control of boost. These components are critical to the stability and efficiency of the hybrid energy system. The general form of the cost

function is:

$$\text{Cost} = \text{MSE}_{\text{battery}} + \text{MSE}_{\text{dq currents}} + \text{MSE}_{\text{DC voltage}}$$

Where:

- $\text{MSE}_{\text{battery}}$ is the MSE of the battery current.
- $\text{MSE}_{\text{dq currents}}$ is the MSE of the dq currents inverter.
- $\text{MSE}_{\text{DC voltage}}$ is the MSE of the boost DC voltage.

The MSE for each component is calculated by averaging the squared differences between the actual values and the reference (desired) values. Mathematically, for any component $y(t)$, the MSE is given by:

$$\text{MSE}(y) = \frac{1}{N} \sum_{t=1}^{N} \left(y(t) - y_{\text{ref}}(t) \right)^2$$

Where:

- $y(t)$ is the actual value of the signal at time t,
- $y_{\text{ref}}(t)$ is the reference value of the signal at time t,
- N is the total number of samples.

4.6 Cost Analysis of the Designed EMS System

The total cost of operating the EMS is calculated by considering various cost components, including the fuel cost of the diesel generator, battery degradation cost, operation and maintenance expenses, unserved energy penalties, and the incentives gained from renewable energy sources. The following paragraphs present the detailed calculation of each component along with their respective contributions to the total cost.

The diesel generator is assumed to operate with a power output of 100 kW for a total of 4 hours. The fuel consumption rate is 0.24 liters per kWh, and the cost of fuel is \$1.2 per liter. Based on these parameters, the total fuel cost is calculated using the formula:

$$C_{\text{fuel}} = P_{\text{DG}} \times T_{\text{op}} \times \text{Fuel Rate} \times \text{Fuel Cost}$$

Substituting the values, we obtain:

$$C_{\text{fuel}} = 100 \times 4 \times 0.24 \times 1.2 = 115.2\,\text{USD}$$

Thus, the total fuel cost for the operation of the diesel generator is \$115.2.

The battery degradation cost is calculated based on the total energy charged and discharged through the battery during the operation. In this case, the energy is 399 kWh, and the degradation cost per unit of energy is \$0.05 per kWh. Using the formula:

$$C_{\text{bat}} = E_{\text{bat}} \times \text{Degradation Cost} \tag{4.10}$$

$$C_{\text{bat}} = 399 \times 0.05 = 19.95\,\text{USD} \tag{4.11}$$

Hence, the battery degradation cost amounts to \$19.95.

The operation and maintenance cost is determined by considering the total system power output, which is 60 kW (daily peak load), and an operation and maintenance cost rate of \$0.01 per kWh. The calculation is as follows:

$$C_{\text{OM}} = P_{\text{sys}} \times T_{\text{op}} \times \text{Operation Maintenance Rate} \tag{4.12}$$

$$C_{\text{OM}} = 60 \times 10 \times 0.01 = 6\,\text{USD} \tag{4.13}$$

The total operation and maintenance cost is therefore \$6.

The cost of unserved energy is calculated based on the unserved demand of 10 kW

and a penalty rate of \$2.0 per kWh. Using the formula:

$$C_{\text{unserved}} = P_{\text{unserved}} \times \text{Penalty Rate} \tag{4.14}$$

$$C_{\text{unserved}} = 10 \times 2.0 = 20\,\text{USD} \tag{4.15}$$

This results in a penalty cost of \$20 due to unserved energy.

Finally, renewable energy incentives are calculated based on the power output from photovoltaic (PV) sources. The PV system generates 60 kW of power over a 10-hour period, with an incentive rate of \$0.02 per kWh. The incentive is given by:

$$B_{\text{RE}} = P_{\text{PV}} \times T_{\text{op}} \times \text{Incentive Rate} = 60 \times 10 \times 0.02 = 12\,\text{USD} \tag{4.16}$$

Thus, the total incentive from renewable energy sources is \$12, which reduces overall cost.

The total cost of the EMS operation is obtained by summing up the individual cost components and subtracting the renewable energy incentives:

$$C_{\text{total}} = C_{\text{fuel}} + C_{\text{bat}} + C_{\text{OM}} + C_{\text{unserved}} - B_{\text{RE}} \tag{4.17}$$

$$C_{\text{total}} = 115.2 + 19.95 + 6 + 20 - 12 = 149.15\,\text{USD} \tag{4.18}$$

Therefore, the total cost of operating the Energy Management System is \$149.15. This analysis demonstrates the cost contributions of various system components and highlights the impact of renewable energy incentives in reducing the overall expenses.

To calculate the cost per kWh, we need the total energy delivered by the system, hence lets calculate as follows.

Energy Delivered by Diesel Generator:

$$E_{\text{DG}} = P_{\text{DG}} \times T_{\text{op}} = 100\,\text{kW} \times 4\,\text{hours} = 400\,\text{kWh} \tag{4.19}$$

Energy Delivered by PV System:

$$E_{\text{PV}} = P_{\text{PV}} \times T_{\text{op}} = 60\,\text{kW} \times 10\,\text{hours} = 600\,\text{kWh} \tag{4.20}$$

Total Energy Delivered:

$$E_{\text{total}} = E_{\text{DG}} + E_{\text{PV}} = 400 + 600 = 1000\,\text{kWh} \tag{4.21}$$

Therefore, to find the cost per kWh, divide the total cost by the total energy delivered:

$$C_{\text{total-per-kWh}} = \frac{C_{\text{total}}}{E_{\text{total}}} = \frac{149.15}{1000} = 0.14915\,\text{USD/kWh} \tag{4.22}$$

Thus, the total cost per kWh of operating the EMS is approximately 0.15 USD/kWh.

Chapter 5

Simulation Results and Analysis

This chapter presents the results and analysis of the simulation for optimizing the design of a hybrid mini-grid system control consisting of diesel generators, solar photovoltaic (PV) panels, and energy storage units. The optimization is achieved using the Bacteria-Foraging Algorithm (BFA). The system is designed to ensure a reliable and cost-effective energy supply. The simulation aims to determine the optimal sizes of the designed controllers to achieve a balance between cost, reliability, and sustainability. The overall simulation data preparation and procedures is outlined in the following sections.

5.1 Simulation Data Preparation

The system was designed and simulated using MATLAB Simulink. To accurately model the performance of the photovoltaic (PV) system, a 24 hour data was treated as a 24 second data with regard to the simulation timeframe and data utilization.

The simulation was based on irradiance data that would typically represent a full 24-hour period. This data captures the variations in direct normal irradiance experienced by the PV panels throughout a typical day 5.1. This comprehensive dataset is essential for understanding how solar energy availability fluctuates throughout the day.

For practical reasons, the 24 hour irradiance data was simulated over a significantly shorter timeframe of 24 seconds. This time compression was achieved by scaling the 24 hour data to fit into a 24 second simulation period. This approach allows the simulation

to maintain a high temporal resolution while condensing the data into a manageable duration. The time compression simulates a full day's worth of irradiance changes within a brief period, facilitating a detailed and rapid analysis of system performance.

Simulating the 24 hour data over a 24 second period provides a detailed view of daily solar irradiance patterns in a compressed format. This method allows for efficient analysis and testing of the PV system's response to typical daily variations in solar energy. Despite the time compression, the simulation retains the essential characteristics of the irradiance data, enabling effective evaluation of system performance and optimization strategies.

In addition, the hourly average power described in figure 3.7 was used as the load profile for simulating over 24 second format. This approach balances the need for detailed daily irradiance patterns with the practical constraints of simulation duration, allowing for efficient and insightful performance analysis.

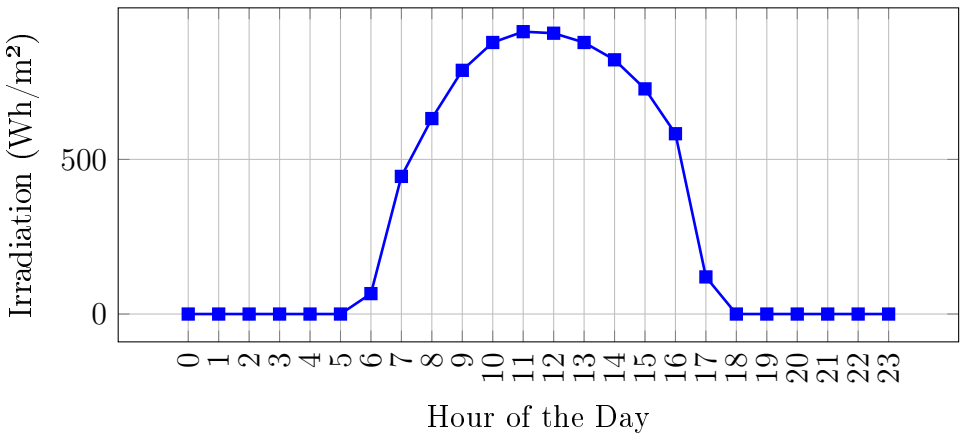

Figure 5.1: Hourly Irradiance Data for February

Simulations are conducted to assess the performance of the hybrid system under various scenarios. The following results provide insights into how well the system meets the energy demand and how the different components contribute to overall performance.

5.2 Results Analysis and Discussion

The results from the simulations are analyzed to determine the optimal sizes of the system components. This analysis includes evaluating the energy production and consumption profiles, cost-effectiveness, and reliability of the system.

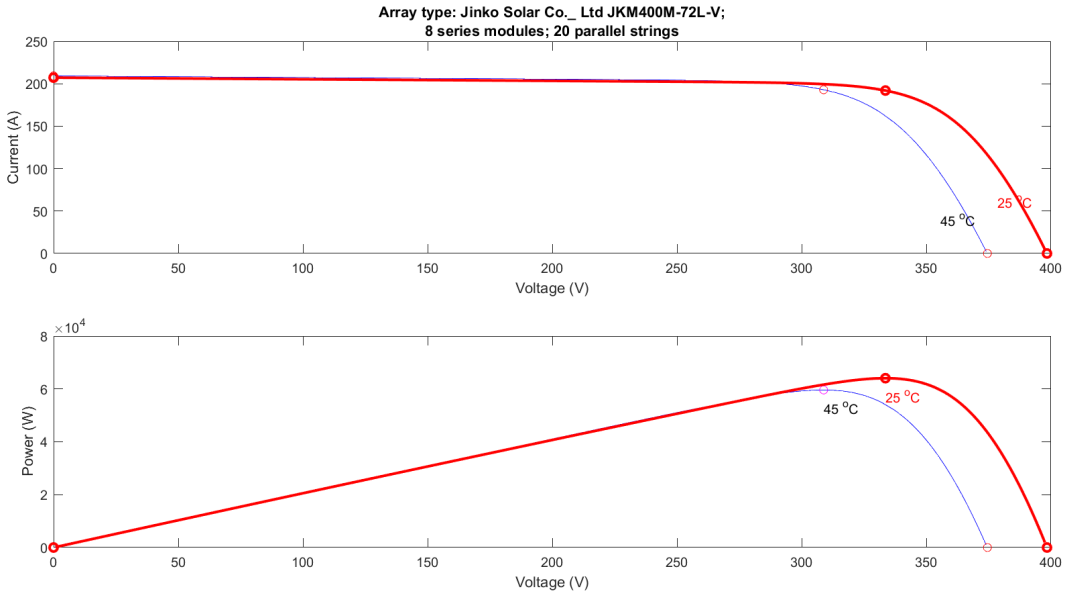

Figure 5.2: Characteristics Curve of the PV Panel

The Figure 5.2 shows the current-voltage (I-V) and power-voltage (P-V) characteristics curve of a photovoltaic (PV) panel. The PV array used is a Jinko Solar of JKM400M-72L-V type, consisting of 8 series modules and 20 parallel strings. The characteristic graph shows how the panel performs under two different temperature conditions, 25°C and 45°C, highlighting the effect of temperature on PV performance. In the I-V curve, current remains almost constant with voltage until a sharp drop occurs as the voltage nears 500 V. This 500 V is the point of maximum system voltage of the mini grid system designed in the process. The P-V curve shows how power initially increases with voltage and reaches a maximum value around 66 kW at 458.7 V for 45°C before sharply decreasing. This 66 kW power and 458.7 V are able to support the peak power of the load profile 54.65 kW with close system voltage value. The differences between the 25°C and 45°C curves illustrate that higher temperatures result in lower power output and

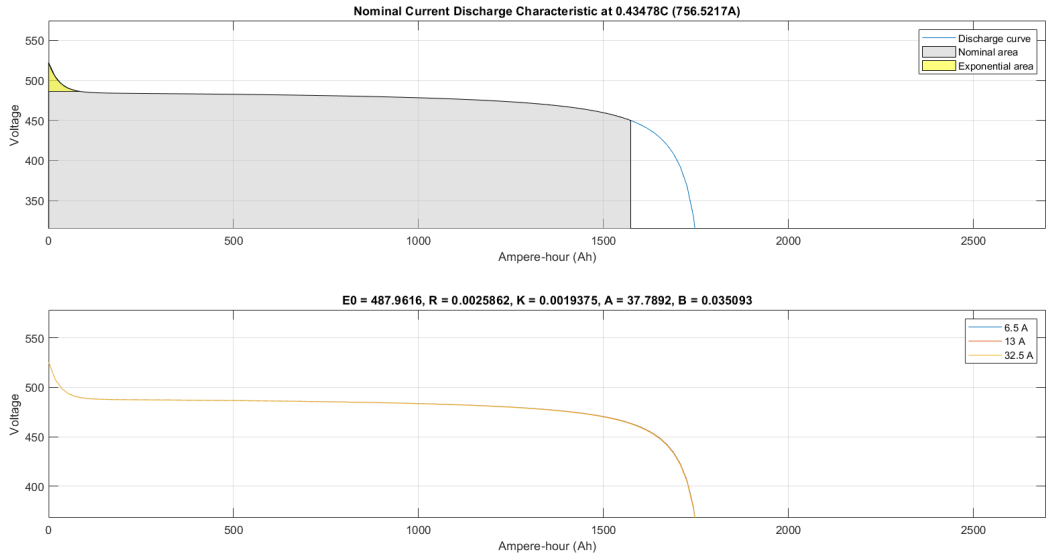

Figure 5.3: Characteristics Curve of the Battery Bank

voltage. This behavior is typical of PV panels and emphasizes the importance of thermal effects in optimizing solar energy system performance.

Figure 5.3 shows the battery performance within the off-grid hybrid system design. The first subplot figure shows the discharge behavior of the battery bank at a nominal current of 756.52A. It shows that the battery is able to provide consistent voltage output over a wide range of Ampere-hours (Ah) before a rapid decline, indicating the end of its charge cycle at around 1720 Ah which is the designed parameter of the battery system. The nominal and exponential areas (shaded regions) are the operational zones where the battery efficiently stores and discharges energy in coordination with other system components of PV and diesel sources. The second subplot figure shows the battery's voltage response at different current levels (6.5A, 13A, 32.5A) which is essential for designing a reliable energy management system. It illustrates how varying loads affect the battery's discharge profile which a critical factor in ensuring continuous power supply when PV generation fluctuates or the diesel generator provides backup. These discharge characteristics are vital for optimizing the energy storage capacity and cycling efficiency of the battery bank.

The PV generated in Figure 5.4 represents the power generated by the PV system over

time. It increases during the daytime when solar irradiance is available and decreases as the day progresses, showing the typical behavior of solar power generation. The battery supplied indicates the power flow to and from the battery storage. Positive values represent charging (when excess PV power is stored), and negative values indicate discharging (when the battery supplies power to meet the demand). The net power in the system is calculated by the sum of all generated and consumed power. It fluctuates based on the balance between generation, storage, and demand. The diesel power depicts the power output of the diesel generator. The generator typically kicks in when the demand exceeds the power available from the PV system and battery storage, often during periods of low solar generation. The load demand represents the power demand of the system. It indicates how the total power generated from PV, battery, and diesel sources is managed to meet the load requirements.

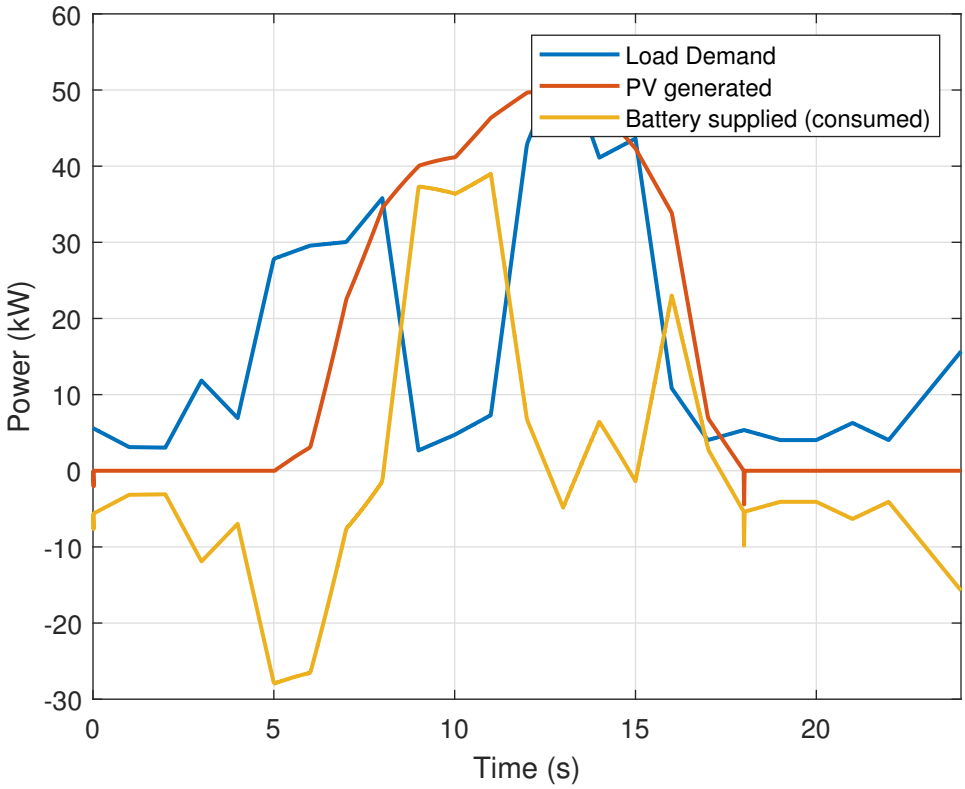

Figure 5.4: Power Distribution in the Energy Management System

From the power distribution Figures 5.4, and 5.5 the following analysis are made. During the day time the PV system generates the majority of the power, with the bat-

tery charging during periods of excess generation. The net power is generally positive, indicating that generation exceeds demand. The diesel generator operates minimally or not at all. As solar power declines the battery starts discharging to meet the demand. The net power become negative, especially as the PV output decreases and when the demand remains high. If the combined output of the PV system and battery storage is insufficient to meet the demand, the diesel generator activates to provide the necessary additional power, as shown by the green line.

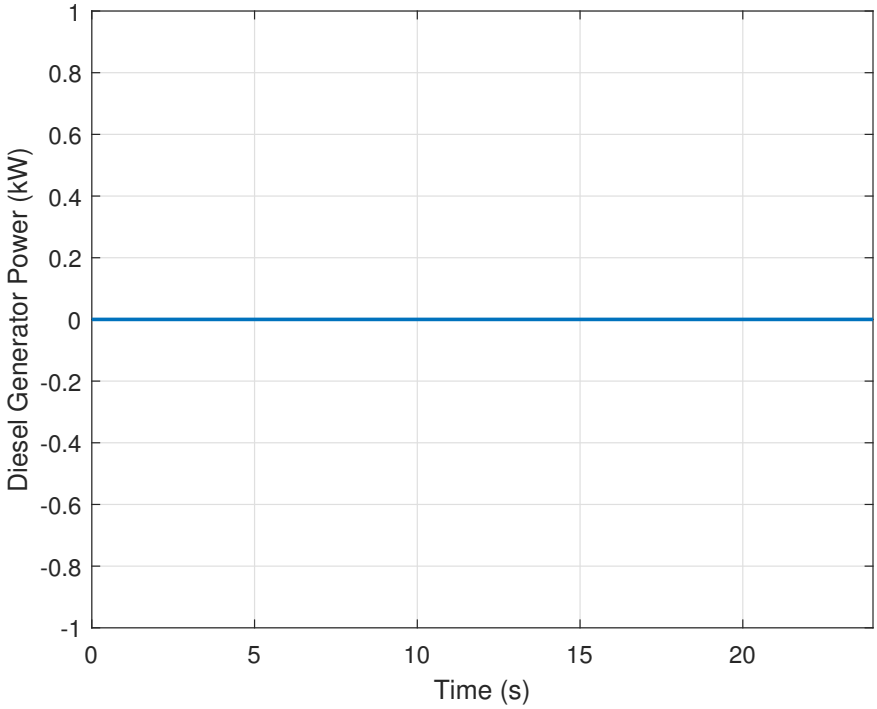

Figure 5.5: Power Distribution in the Diesel Generator

Finally, the goal is to maximize the use of PV power and battery storage while minimizing diesel generator use. The efficiency of this system design is reflected in how well it manages these power sources to meet demand with minimal diesel consumption. Hence, the figure is essential for understanding how the hybrid system balances renewable energy generation, storage, and traditional energy sources to maintain a reliable power supply in an off-grid scenario.

The battery charging and discharging control system gives the reasonable and satisfactory results, given in Figures 5.6,5.7, 5.8, and 5.9. The battery current control depicted

in Figure 5.6 demonstrates that the current tracks the reference within a very short time of 0.01 seconds, which is feasible for practical applications. This quick response indicates a highly responsive control system, suitable for practical applications where fast and accurate control is essential. The ability to track current so efficiently ensures that the battery operates within safe limits, preventing overcharging or excessive discharging, which could damage the battery or reduce its lifespan.

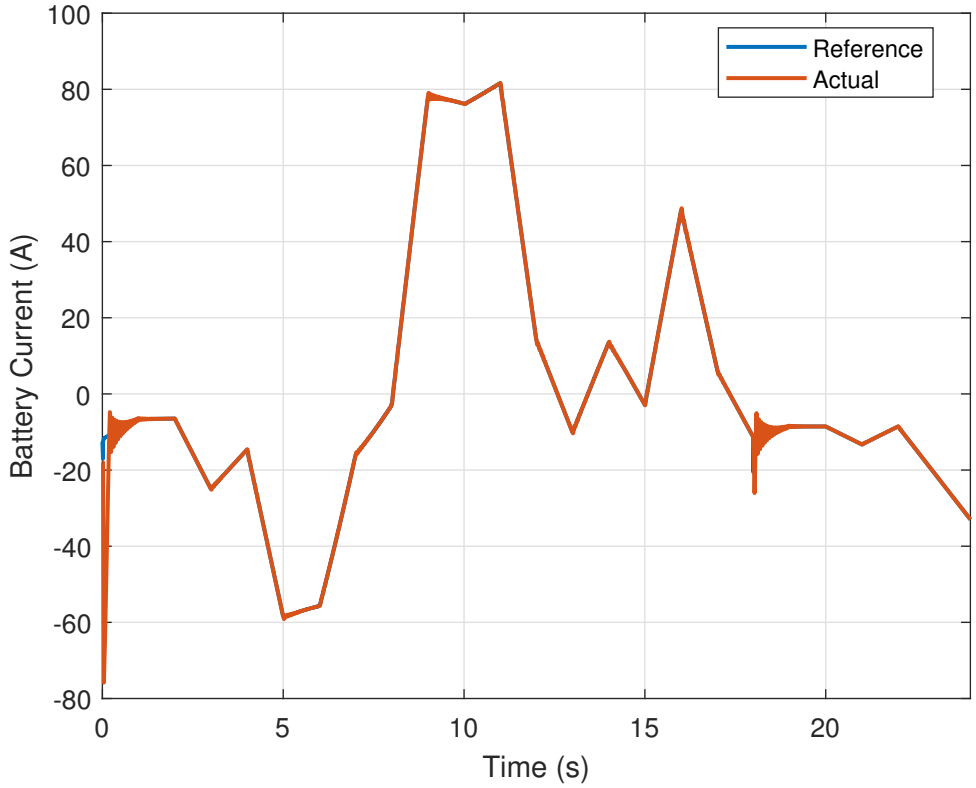

Figure 5.6: Battery Current for the Given Load Profile

Figure 5.7 is about the regulated voltage of the battery through the PI current controller. As it shows, the value of the battery voltage sustains at 477 volts, which is slightly higher than its nominal value of 450 volts but lower than the grid reference DC voltage of 500 volts. This range of operation is recommended for hybrid off-grid system design, ensuring optimal performance and stability in managing the energy flow between the battery and the grid. The result emphasizes that the system is designed to operate efficiently within these limits, protecting the battery from overcharging or undercharging.

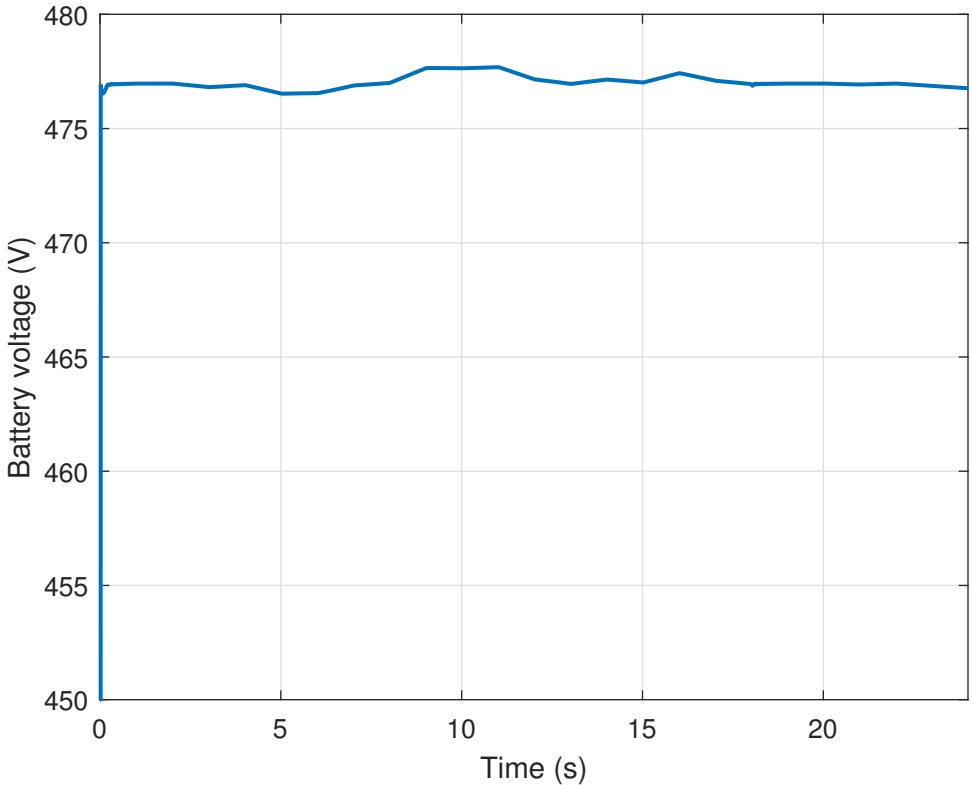

Figure 5.7: Battery Voltage for the Given Load Profile

Figure 5.8 shows the battery's State of Charge (SOC) regulated at a value of 50%. The graph illustrates that the desired SOC of 50% is consistently maintained through the current control command that was designed earlier. This ensures that the battery remains within the optimal SOC range, which is crucial for efficient energy management in hybrid systems. The vertical variation of the SOC from the desired 50% is minimal, with deviations kept within four decimal places. This level of precision highlights the effectiveness of the control strategy, ensuring that fluctuations are negligible and the system operates stably. Such accurate SOC regulation is vital to prolonging the battery's life and maintaining system reliability.

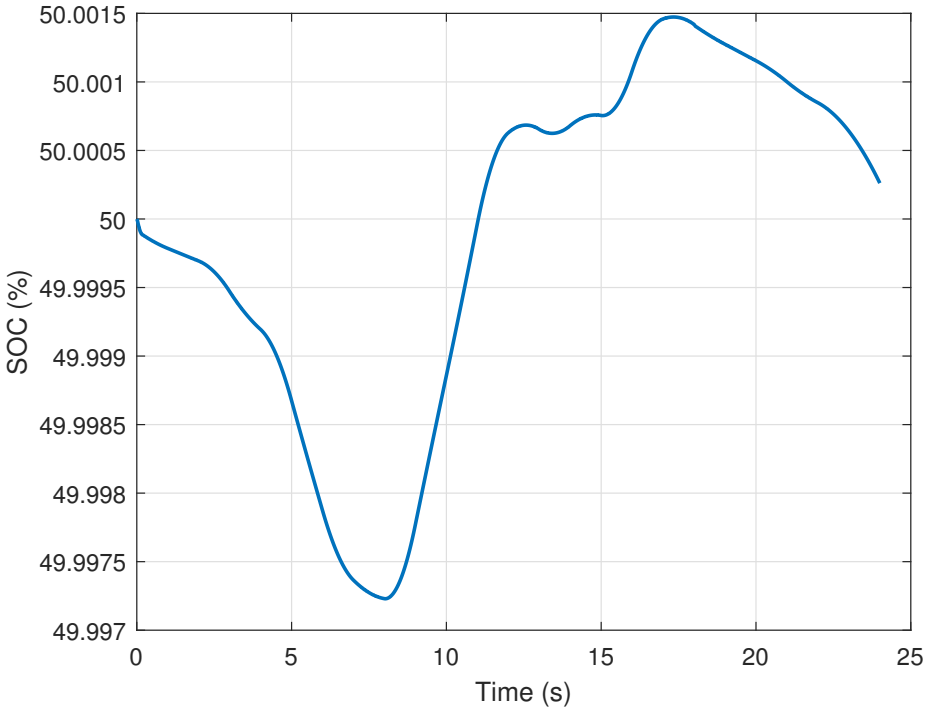

Figure 5.8: Battery SOC Regulation at 50% Value

Figure 5.9 illustrates the successful generation of the duty cycle within a range of values from 0 to 1. The duty cycle is a crucial parameter in controlling the operation of power converters, and its proper regulation ensures efficient energy transfer. The generated duty cycle consistently averages around 0.95, indicating that the system is operating in the upper bound region of its capabilities. This high duty cycle value signifies that the converter is effectively driving power to the load, thereby optimizing the performance of the battery charging and discharging process.

The concentration of the duty cycle near the upper limit suggests that the control system is effectively utilizing the available power while avoiding potential overloading conditions. It highlights the ability of the control algorithm to adapt to changing operational conditions and maintain the desired performance. Such precision in duty cycle generation is vital for enhancing the efficiency of hybrid systems, ensuring that the system operates within safe parameters while maximizing energy output and maintaining battery health.

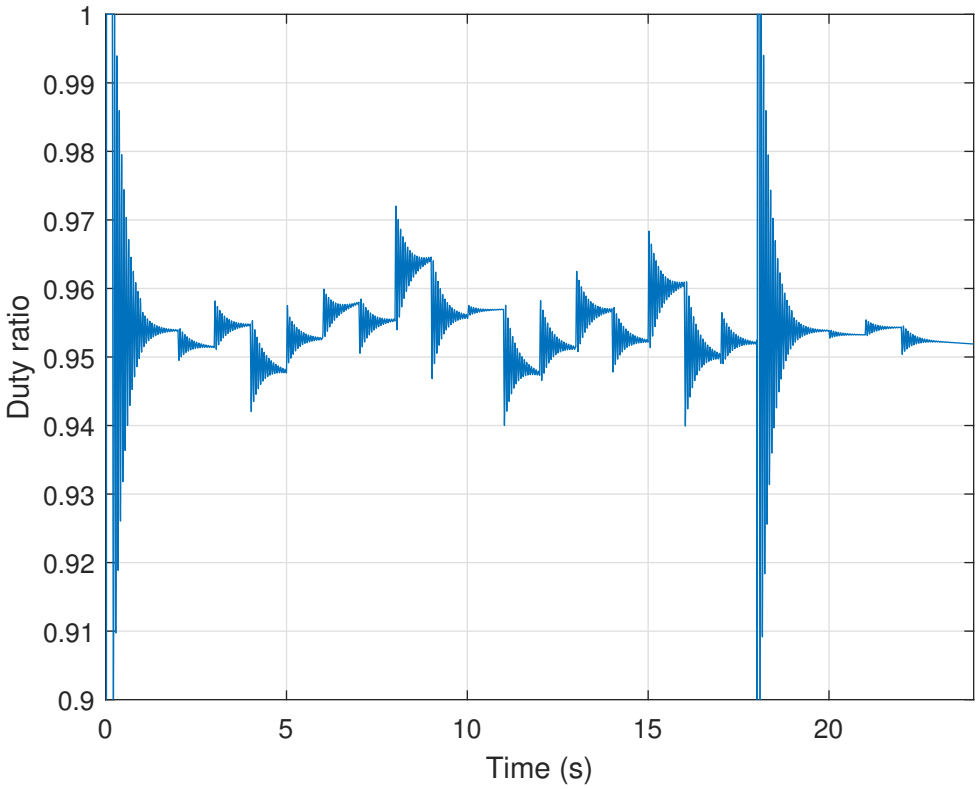

Figure 5.9: Duty Cycle Generation in Battery Control System

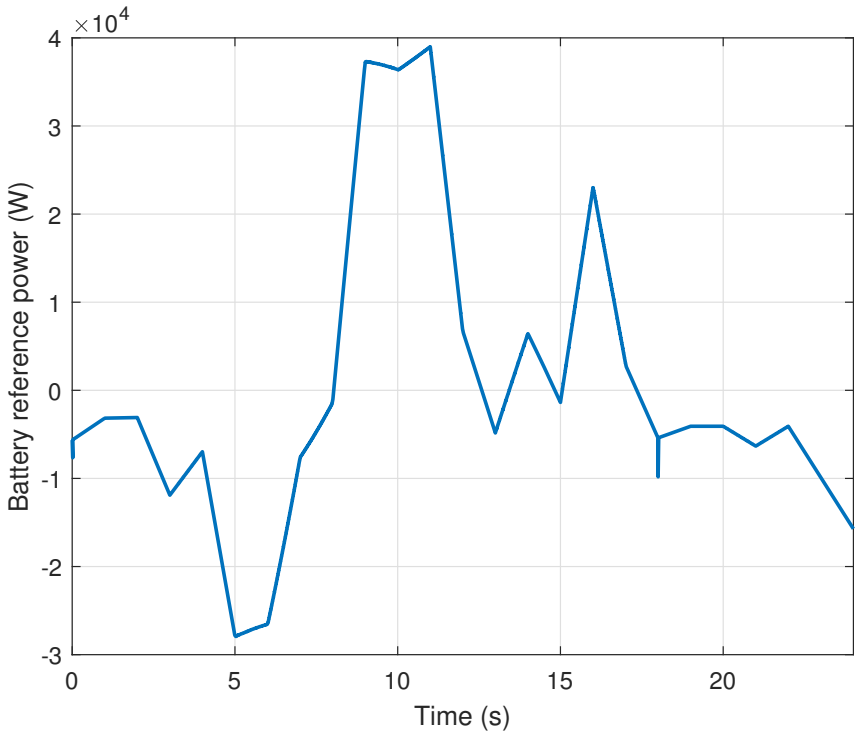

Figure 5.10: Power Distribution of Battery Control System

The boost control system demonstrates satisfactory performance, as illustrated in Figures 5.11, 5.12, and 5.14. Figure 5.11 indicates that the input voltage to the DC/DC boost converter is effectively maintained within a range of 200 to 300 volts during the time horizon of 6 to 17 hours, which corresponds to the non-zero irradiation region. This regulation is crucial for ensuring that the boost converter operates efficiently and reliably, in renewable energy applications where input voltage fluctuate significantly due to varying solar irradiation levels. The successful regulation of both input and output voltages demonstrates the robustness of the control strategy implemented in the boost converter, highlighting its capability to handle dynamic operating conditions while ensuring stable energy conversion.

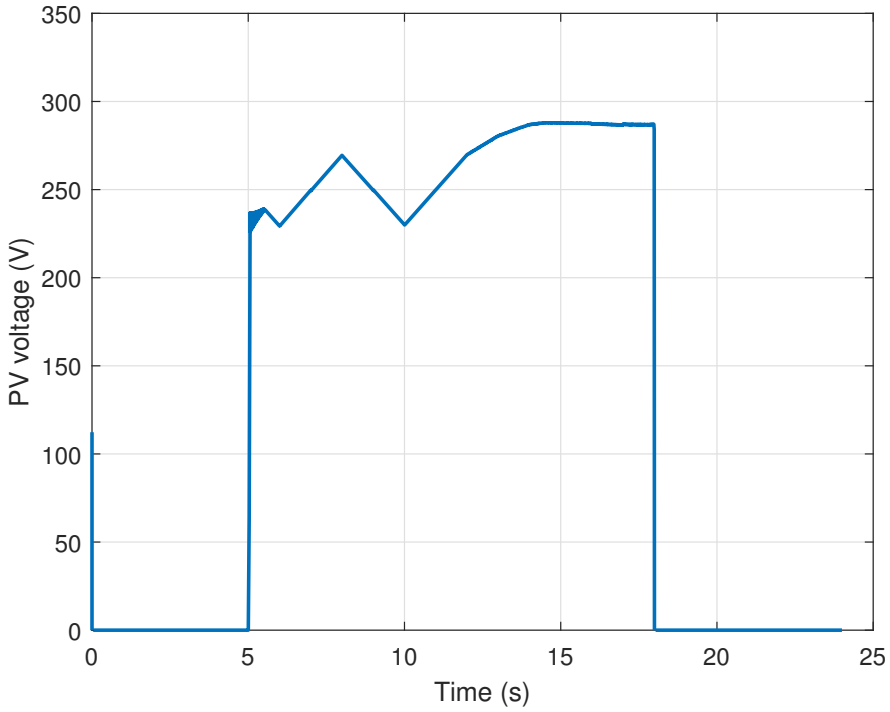

Figure 5.11: Boost Converter Input Voltage from PV Source

Figure 5.12 presents the duty cycle of the boost converter, which is effectively maintained within a range of 0.4 to 0.6. This range indicates that the control system is adept at regulating the duty cycle to optimize the performance of the boost converter. The duty cycle is a critical parameter in DC/DC converters, determining the ratio of the on-time to the total time of the switching cycle. A duty cycle within this range ensures

that the converter can efficiently boost the input voltage to the desired output level of 500 volts.

The observed duty cycle values signify the converter's ability to adapt to varying input conditions while still achieving the necessary output voltage. By operating within the specified duty cycle range, the boost converter effectively manage power flow, minimize losses, and enhance overall system efficiency. This performance is important where fluctuations in input voltage can occur. The precise control of the duty cycle demonstrates the effectiveness of the implemented control strategy, ensuring that the converter operates optimally across different operating conditions.

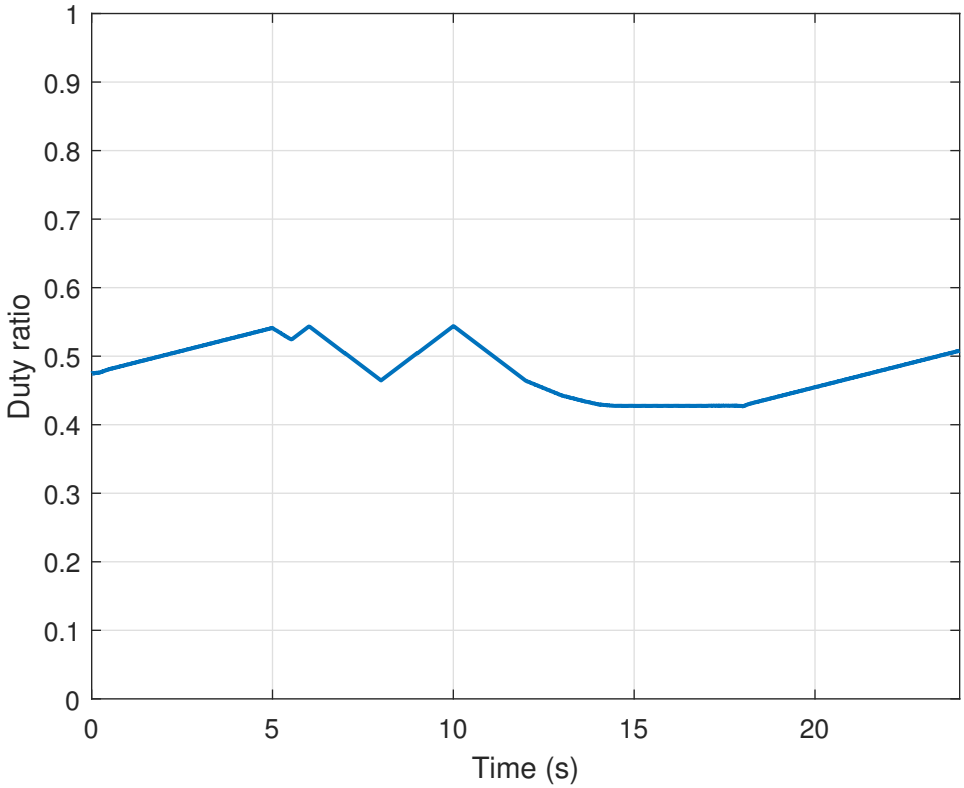

Figure 5.12: Duty Cycle Generation in Boost Converter Control System

The inverter voltage regulation and current control are effectively demonstrated in Figures 5.13, 5.14, and 5.15. In Figure 5.13, the bus voltage is successfully maintained at the desired level of 500 volts. The graph indicates a rapid response to changes in load conditions, showcasing the inverter's ability to adapt quickly and ensure voltage stability. This performance is critical in hybrid systems, where maintaining a consistent voltage is

essential for the reliable operation of connected devices and overall system performance.

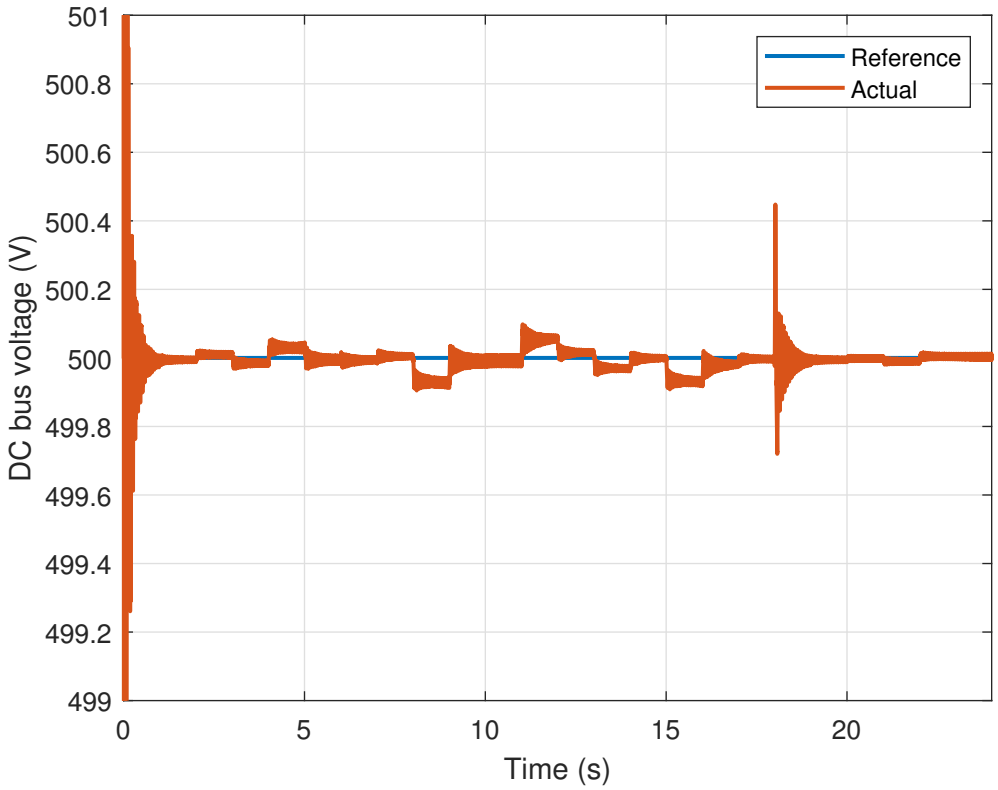

Figure 5.13: Inverter DC Bus Voltage Regulation

Figures 5.14 and 5.15 illustrate the successful tracking of the reference q-axis and d-axis currents. Both figures show that the desired current values were achieved within a brief response time of 0.05 seconds, indicating effective control dynamics. The precise tracking of these currents is crucial for optimal inverter performance, as it directly influences the power flow and operational efficiency. The minimal deviation from the reference currents suggests a well-tuned control algorithm, capable of maintaining system stability and responsiveness in varying operational scenarios. Overall, these figures highlight the robustness of the control strategy implemented in the inverter system.

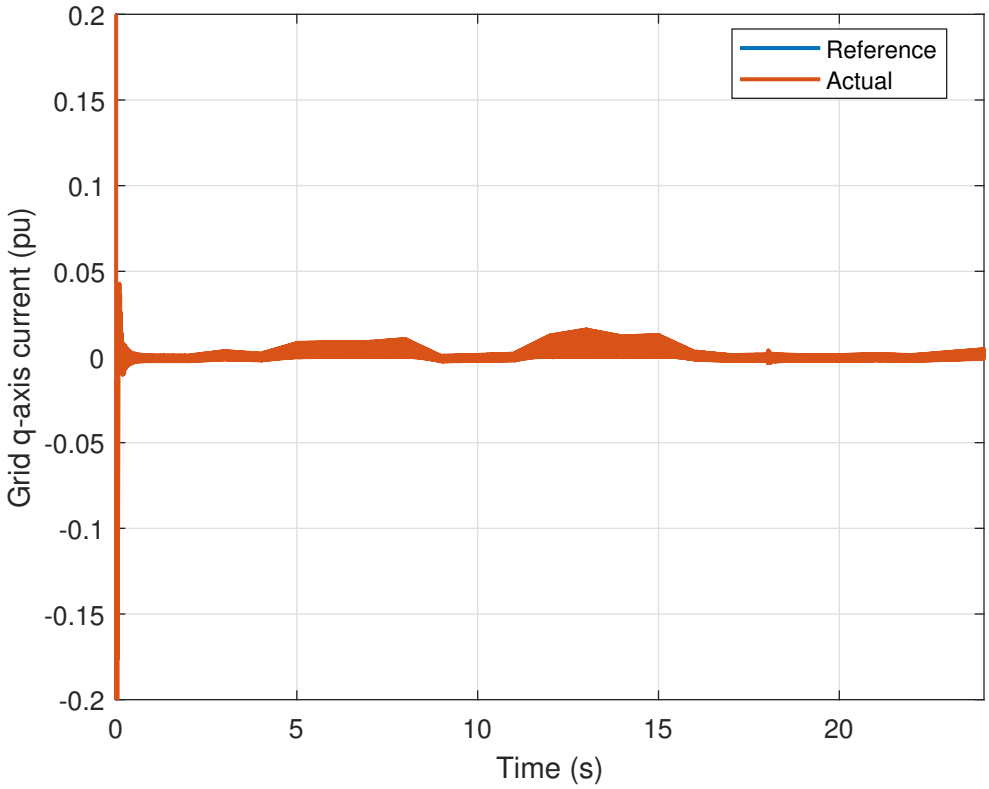

Figure 5.14: Inverter q-axis Current Control

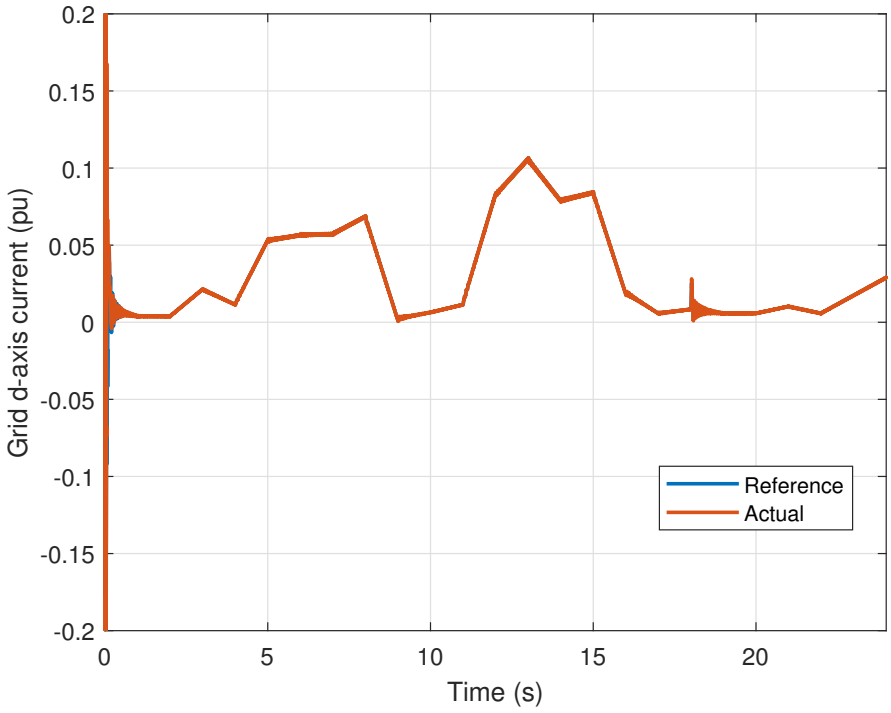

Figure 5.15: Inverter d-axis Current Control

The response of the AC grid was recorded during these simulation scenarios giving the following results. For graphical illustration the grid voltage, current, and power are presented here in Figures 5.16, 5.17, 5.18, 5.20, and 5.19a.

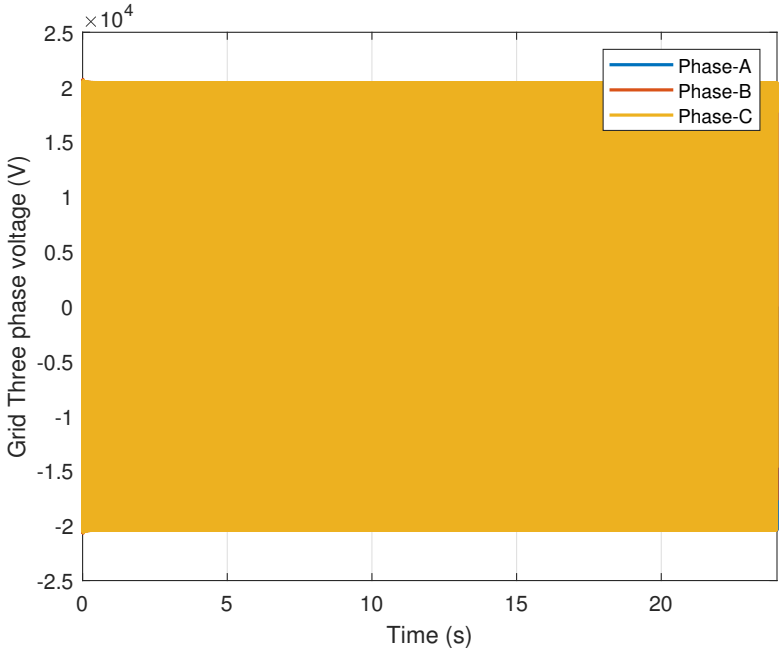

Figure 5.16: Grid Voltage

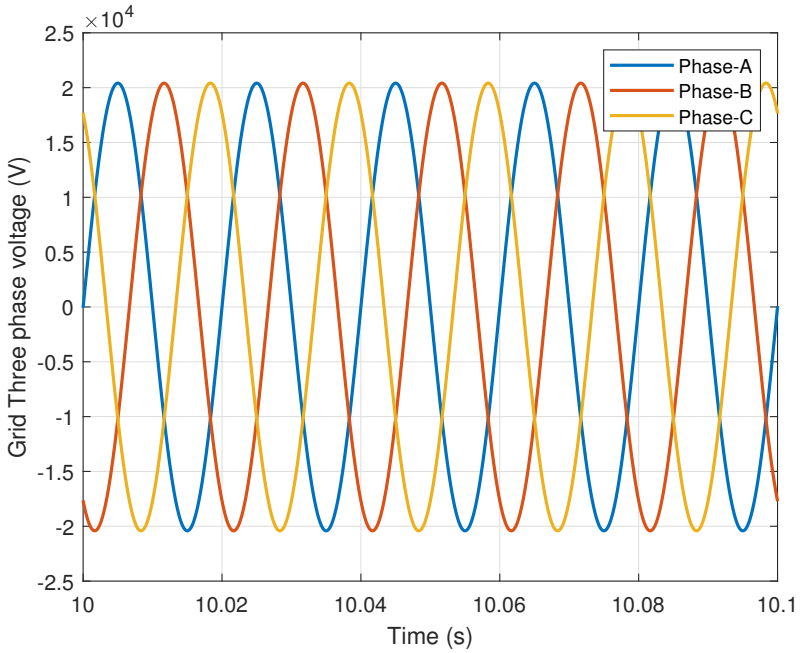

Figure 5.17: Zoom View of Grid Voltage

Figure 5.17 illustrates a zoomed view of the grid voltage for the three phases (Phase-A, Phase-B, and Phase-C) within the solar-diesel hybrid system. The graph demonstrates the behavior of the grid voltage over a short time frame, specifically from 10.00 to 10.10 seconds. The three-phase voltage wave forms exhibit a sinusoidal pattern typical of balanced systems, with voltage levels oscillating around a peak value, indicating effective voltage regulation in the system. The phase voltages remain relatively synchronized, suggesting that the control mechanisms in place successfully maintain a stable voltage output, which is essential for the reliable operation of hybrid power systems.

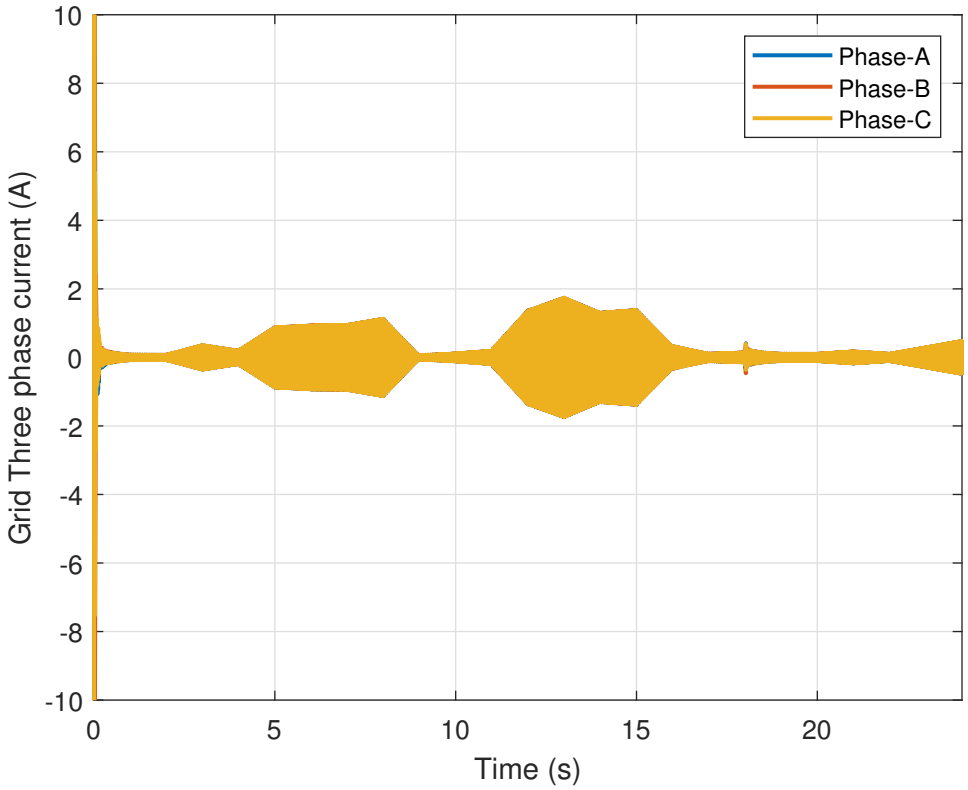

Figure 5.18: Grid Current

Figure 5.18 shows the three-phase grid current over a broader time frame, from 0 to 24 seconds. The current wave forms reveal fluctuations that reflect the dynamic nature of the system, particularly during periods of varying load conditions. The current remains within a manageable range, and the transitions between different phases are smooth, suggesting effective current control. The steady state performance observed in the later sections of the graph indicates that the hybrid system is capable of providing a

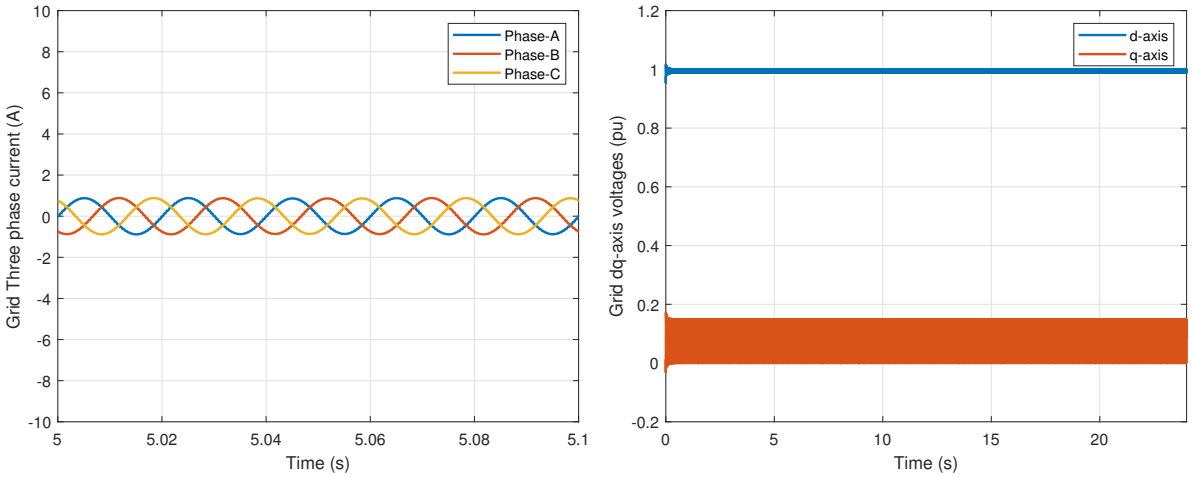

(a) Zoomed View of Grid Current **(b)** Grid Voltage in the d-q Axis

Figure 5.19: (a) Zoomed View of Grid Current (b) Grid Voltage in the d-q Axis

stable power supply, even amidst fluctuations, ensuring reliability and efficiency in energy distribution.

This Figure 5.19b illustrates the grid voltage components along the d-axis and q-axis in a synchronous reference frame for the hybrid mini-grid system. The d-axis voltage remains steady at around 1 per unit (pu) throughout the 24-second time period. This stability suggests that the system is effectively maintaining its active power flow, as the d-axis is responsible for controlling the active power in hybrid systems. On the other hand, the q-axis voltage is consistently around 0.2 pu. The q-axis in a d-q transformation framework is associated with reactive power. The slight difference from zero indicates a small but constant amount of reactive power in the system exists. Moreover, the stability of both voltage components indicates that the control system which is a Voltage Source Converter (VSC), is regulating the grid voltages effectively, ensuring a balanced and reliable operation of the hybrid mini-grid system.

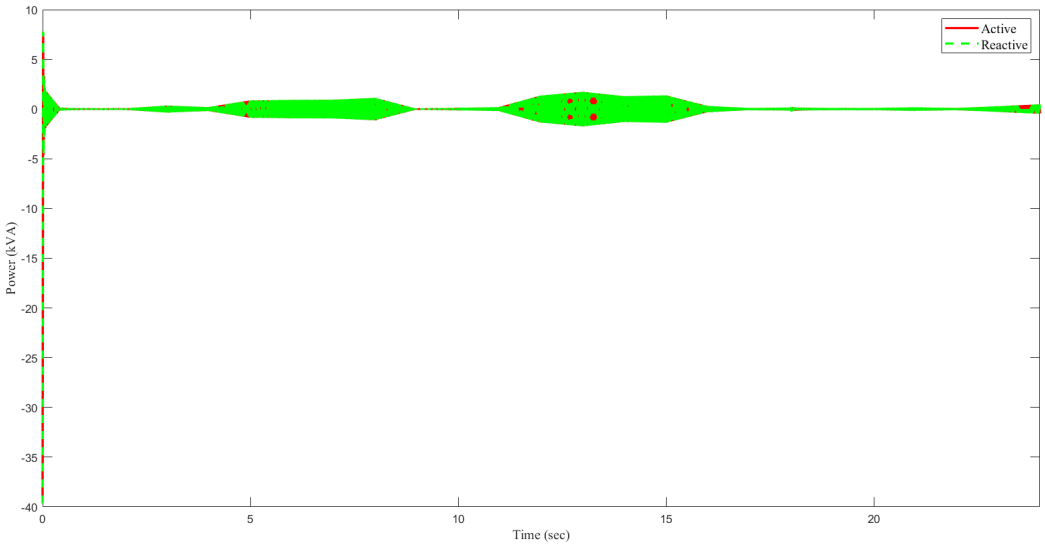

Figure 5.20: Grid Power

Figure 5.20 shows the variation of active power and reactive power over time for the hybrid mini-grid system. Initially, both active and reactive power experience fluctuations, which is attributed to dynamic transitions in the power system. These fluctuations are due to changes in power generation from solar panels, and diesel generators. As the system stabilizes after 6 seconds, both power components reach a steady-state condition, indicating that the control strategy is successfully managing the power flow. The steady active power level suggests that the system is meeting the load demand efficiently, while the reactive power stabilizes at a low level, indicating minimal reactive power exchange. This behavior is essential for off-grid hybrid systems, as it highlights the system's ability to balance multiple energy sources while ensuring efficient and stable power supply to the grid. The combination of solar panel, battery system and diesel power, along with effective power management, provides reliable energy for remote and off-grid areas.

Chapter 6

Conclusion and Recommendation

6.1 Conclusion

The simulation results presented in this thesis demonstrate the effectiveness of the proposed hybrid mini-grid system, which integrates diesel generators, solar photovoltaic (PV) panels, and energy storage units, optimized using the Bacteria-Foraging Algorithm (BFA). The system successfully balances the trade-offs between using these different energy sources. The following key conclusions are drawn from the simulation results.

The power management system effectively regulates the flow of power between the PV system, battery storage, and diesel generators, ensuring that energy demand is met with minimal reliance on diesel. The PV system effectively harnesses solar energy during daylight hours, minimizing the need for diesel generators and battery banks. The battery storage system efficiently stores excess energy and supplies power during periods of low solar irradiance.

The battery charging and discharging control system exhibits rapid response times, with battery current control achieving steady-state within 0.01 seconds. The battery voltage remains within the recommended operating range, sustaining at approximately 483 volts. The boost converter effectively maintains the desired DC output voltage of 500 volts during periods of active solar generation, with duty cycle regulation achieved within the specified range of 0.4 to 0.6. The inverter control system exhibits satisfactory performance, with bus voltage regulation and current control tracking the desired

reference values within 0.05 seconds, ensuring stable power conversion and distribution.

Furthermore, the hybrid mini-grid system demonstrates a high level of efficiency and reliability in managing renewable energy resources, thereby reducing dependency on diesel generators and enhancing the sustainability of off-grid power supply systems.

6.2 Recommendation

Based on the simulation results, the following recommendations are proposed for further improvement and practical implementation in the future works.

- Future work shall focus on refining the sizing of system components, particularly the battery storage capacity and PV panel array, to further optimize cost-effectiveness while maintaining system reliability.
- The BFA has proven effective, while exploring other advanced optimization algorithms such as Genetic Algorithms (GA) or Particle Swarm Optimization (PSO) could yield further improvements in system performance.
- Integrating real-time data inputs, such as live solar irradiance and load demand, into the control system could enhance the adaptability and responsiveness of the hybrid mini-grid system under dynamic environmental conditions.
- To validate the simulation results, it is recommended to implement the proposed system in a real-world setting, as a pilot project in a remote off-grid location.
- Future research can consider the scalability of the system to accommodate larger loads or expanded service areas, as well as the flexibility to integrate additional renewable energy sources, of wind or biomass, to further enhance system sustainability.

References

[1] R. U. Ayres and B. Warr, *The economic growth engine: how energy and work drive material prosperity.* Edward Elgar Publishing, 2010.

[2] A. W. Kassie, S. W. Mengistu *et al.*, "Spatiotemporal analysis of the proportion of unimproved drinking water sources in rural ethiopia: Evidence from ethiopian socioeconomic surveys (2011 to 2019)," *Journal of Environmental and Public Health*, vol. 2022, 2022.

[3] Y. Mohammed, M. Mustafa, and N. Bashir, "Hybrid renewable energy systems for off-grid electric power: Review of substantial issues," *Renewable and Sustainable Energy Reviews*, vol. 35, pp. 527–539, 2014.

[4] O. GUMISIRIZA, "Optimal sizing and techno-economic analysis of a stand-alone photovoltaic–wind hybrid system: A case study of busitema health centre iii in busia district, eastern uganda," Master's thesis, PAUWES, 2020.

[5] G. Bekele and G. Boneya, "Design of a photovoltaic-wind hybrid power generation system for ethiopian remote area," *energy Procedia*, vol. 14, pp. 1760–1765, 2012.

[6] F. Bekele, "Feasibility study of power generation using off-grid energy system from micro hydro-pv-diesel generator-battery for rural area of ethiopia: The case of indris river, western ethiopia," *Western Ethiopia (Doctoral dissertation, Addis Ababa University Addis Ababa, Ethiopia)*, 2017.

[7] D. Chen, "Control and operation of a dc microgrid," Ph.D. dissertation, Queen's University Belfast, 2012.

[8] S. Malla and C. Bhende, "Voltage control of stand-alone wind and solar energy system," *International Journal of Electrical Power & Energy Systems*, vol. 56, pp. 361–373, 2014.

[9] A. Halim, A. Fudholi, S. Phillips, and K. Sopian, "Review on optimised configuration of hybrid solar-pv diesel system for off-grid rural electrification." *International Journal of Power Electronics and Drive Systems*, vol. 9, no. 3, p. 1374, 2018.

[10] G. S. Kantibhai and S. Kumar, "Performance analysis of inc based mppt for pv system."

[11] A. A. Bensaber, M. Benghanem, A. Guerouad, and M. A. Bensaber, "Power flow control and management of a hybrid power system," *Przeglad Elektrotechniczny*, vol. 1, no. 1, pp. 188–192, 2019.

[12] M. Nagaiah and K. C. Sekhar, "Analysis of fuzzy logic controller based bi-directional dc-dc converter for battery energy management in hybrid solar/wind micro grid system," *International Journal of Electrical and Computer Engineering*, vol. 10, no. 3, p. 2271, 2020.

[13] A. Addis, "Fuzzy logic controller based maximum power tracking for hybrid solar/wind power generation case study on debre tsion island," Ph.D. dissertation, 2020.

[14] N. Yimen, O. Hamandjoda, L. Meva'a, B. Ndzana, and J. Nganhou, "Analyzing of a photovoltaic/wind/biogas/pumped-hydro off-grid hybrid system for rural electrification in sub-saharan africa—case study of djoundé in northern cameroon," *Energies*, vol. 11, no. 10, p. 2644, 2018.

[15] Y. Abou Jieb, E. Hossain, Y. Abou Jieb, and E. Hossain, "Solar system components," *Photovoltaic Systems: Fundamentals and Applications*, pp. 95–192, 2022.

[16] A. S. Ingole, B. S. Rakhonde *et al.*, "Hybrid power generation system using wind energy and solar energy," *International Journal of Scientific and Research Publications*, vol. 5, no. 3, pp. 1–4, 2015.

[17] E. M. Natsheh, "Hybrid power systems energy management based on artificial intelligence," Ph.D. dissertation, Manchester Metropolitan University, 2013.

[18] A. Maheri, "Multi-objective design optimisation of standalone hybrid wind-pv-diesel systems under uncertainties," *Renewable Energy*, vol. 66, pp. 650–661, 2014.

[19] J. B. Alonso, P. Sandwell, and J. Nelson, "The potential for solar-diesel hybrid mini-grids in refugee camps: A case study of nyabiheke camp, rwanda," *Sustainable Energy Technologies and Assessments*, vol. 44, p. 101095, 2021.

[20] S. S. Yusuf and N. N. Mustafi, "Design and simulation of an optimal mini-grid solar-diesel hybrid power generation system in a remote bangladesh," *International Journal of Smart Grids, ijSmartGrid*, vol. 2, no. 1, pp. 27–33, 2018.

[21] M. A. Shoeb, T. Jamal, G. Shafiullah, and M. M. Rahman, "Analysis of remote pv-diesel based hybrid minigrid for different load conditions," in *2016 IEEE Innovative Smart Grid Technologies-Asia (ISGT-Asia)*. IEEE, 2016, pp. 1165–1170.

[22] E. I. C. Zebra, H. J. van der Windt, G. Nhumaio, and A. P. Faaij, "A review of hybrid renewable energy systems in mini-grids for off-grid electrification in developing countries," *Renewable and Sustainable Energy Reviews*, vol. 144, p. 111036, 2021.

[23] G. Shafiullah and C. E. Carter, "Feasibility study of photovoltaic (pv)-diesel hybrid power systems for remote networks," in *2015 IEEE Innovative Smart Grid Technologies-Asia (ISGT ASIA)*. IEEE, 2015, pp. 1–7.

[24] K. K. Jasim, M. A. Abdul-hussien, and E. M. Sarhan, "Design of hybrid solar pv diesel mini grids in iraq," *journal of the college of basic education*, vol. 21, no. 90, pp. 109–128, 2015.

[25] S. A. Chowdhury, S. Aziz, S. Groh, H. Kirchhoff, and W. Leal Filho, "Off-grid rural area electrification through solar-diesel hybrid minigrids in bangladesh: resource-efficient design principles in practice," *Journal of cleaner production*, vol. 95, pp. 194–202, 2015.

[26] T. M. Razykov, C. S. Ferekides, D. Morel, E. Stefanakos, H. S. Ullal, and H. M. Upadhyaya, "Solar photovoltaic electricity: Current status and future prospects," *Solar energy*, vol. 85, no. 8, pp. 1580–1608, 2011.

[27] A. K. Pandey, V. Tyagi, A. Jeyraj, L. Selvaraj, N. Rahim, and S. Tyagi, "Recent advances in solar photovoltaic systems for emerging trends and advanced applications," *Renewable and Sustainable Energy Reviews*, vol. 53, pp. 859–884, 2016.

[28] F. Akarslan, "Photovoltaic systems and applications," *Modeling and Optimization of Renewable Energy Systems*, vol. 3, pp. 1035–1041, 2012.

[29] F. A. Khan, N. Pal, and S. H. Saeed, "Review of solar photovoltaic and wind hybrid energy systems for sizing strategies optimization techniques and cost analysis methodologies," *Renewable and Sustainable Energy Reviews*, vol. 92, pp. 937–947, 2018.

[30] M. D. Al-Falahi, S. Jayasinghe, and H. Enshaei, "A review on recent size optimization methodologies for standalone solar and wind hybrid renewable energy system," *Energy conversion and management*, vol. 143, pp. 252–274, 2017.

[31] R. Posadillo and R. L. Luque, "Approaches for developing a sizing method for stand-alone pv systems with variable demand," *Renewable Energy*, vol. 33, no. 5, pp. 1037–1048, 2008.

[32] J. Li, "Optimal sizing of grid-connected photovoltaic battery systems for residential houses in australia," *Renewable energy*, vol. 136, pp. 1245–1254, 2019.

[33] A. G. Abo-Khalil, K. Sayed, A. Radwan, and I. A. El-Sharkawy, "Analysis of the pv system sizing and economic feasibility study in a grid-connected pv system," *Case Studies in Thermal Engineering*, vol. 45, p. 102903, 2023.

[34] A. Jossen, J. Garche, and D. U. Sauer, "Operation conditions of batteries in pv applications," *Solar energy*, vol. 76, no. 6, pp. 759–769, 2004.

[35] S. Kumar and A. Sharma, "Optimizing sizing of pv systems for peak load demands in remote locations," *Energy Reports*, vol. 6, pp. 315–325, 2020.

[36] J. Singh and S. Prasad, "Sizing of hybrid systems: A practical approach to meet the peak load demands of remote locations," in *Proceedings of the International Conference on Renewable Energy*, Delhi, India, 2019, pp. 128–135.

[37] J. Wen, D. Zhao, and C. Zhang, "An overview of electricity powered vehicles: Lithium-ion battery energy storage density and energy conversion efficiency," *Renewable Energy*, vol. 162, pp. 1629–1648, 2020.

[38] F. G. Üçtuğ and A. Azapagic, "Environmental impacts of small-scale hybrid energy systems: Coupling solar photovoltaics and lithium-ion batteries," *Science of the total environment*, vol. 643, pp. 1579–1589, 2018.

[39] T. Chen, Y. Jin, H. Lv, A. Yang, M. Liu, B. Chen, Y. Xie, and Q. Chen, "Applications of lithium-ion batteries in grid-scale energy storage systems," *Transactions of Tianjin University*, vol. 26, no. 3, pp. 208–217, 2020.

[40] V. SHARMA, "Energy storage system and its use with renewable energy."

[41] T. Chen, Y. Jin, H. Lv, A. Yang, M. Liu, B. Chen, Y. Xie, and Q. Chen, "Applications of lithium-ion batteries in grid-scale energy storage systems," *Transactions of Tianjin University*, vol. 26, no. 3, pp. 208–217, 2020.

[42] L. Zhang and X. Xiong, "The soc estimation of a lead acid rechargeable battery," in *Innovations and Advances in Computing, Informatics, Systems Sciences, Networking and Engineering*. Springer, 2015, pp. 503–508.

[43] F. Ciancetta, E. Fiorucci, A. Fioravanti, S. Mari, A. Prudenzi, A. Silvestri *et al.*, "System for repetitive battery charge and discharge tests for battery life analysis," *RE&PQJ*, vol. 20, no. 1, 2022.

[44] ——, "System for repetitive battery charge and discharge tests for battery life analysis," *RE&PQJ*, vol. 20, no. 1, 2022.

[45] O. Style, *Stand-Alone Solar Energy: Planning, sizing and installation of Stand-alone photovoltaic systems*. Oliver Style, 2013.

[46] W. Ali, H. Farooq, A. U. Rehman, Q. Awais, M. Jamil, and A. Noman, "Design considerations of stand-alone solar photovoltaic systems," in *2018 International conference on computing, electronic and electrical engineering (ICE Cube)*. IEEE, 2018, pp. 1–6.

[47] M. A. Ramli, A. Hiendro, and S. Twaha, "Economic analysis of pv/diesel hybrid system with flywheel energy storage," *Renewable Energy*, vol. 78, pp. 398–405, 2015.

[48] I. Din, M. A. Rosen, P. Ahmadi *et al.*, *Optimization of energy systems*. John Wiley & Sons, 2017.

[49] Ø. Skarstein and K. Uhlen, "Design considerations with respect to long-term diesel saving in wind/diesel plants," *Wind engineering*, pp. 72–87, 1989.

[50] B. Bala and S. A. Siddique, "Optimal design of a pv-diesel hybrid system for electrification of an isolated island—sandwip in bangladesh using genetic algorithm," *Energy for sustainable Development*, vol. 13, no. 3, pp. 137–142, 2009.

[51] Z. Iqbal, G. Soyumer, and W. Kazim, "Design and implementation of 59 kwp solar hybrid mini-grid in solab, ras al khaimah," in *2014 IEEE 40th Photovoltaic Specialist Conference (PVSC)*. IEEE, 2014, pp. 2743–2747.

[52] A. Zein and G. Bazzoun, "Integration of photovoltaic generators into existing diesel mini-grids in lebanon," in *2013 25th International Conference on Microelectronics (ICM)*. IEEE, 2013, pp. 1–4.

[53] A. Chauhan and R. Saini, "A review on integrated renewable energy system based power generation for stand-alone applications: Configurations, storage options, sizing methodologies and control," *Renewable and Sustainable Energy Reviews*, vol. 38, pp. 99–120, 2014.

[54] S. Ahmad, M. Z. A. Ab Kadir, and S. Shafie, "Current perspective of the renewable energy development in malaysia," *Renewable and sustainable energy reviews*, vol. 15, no. 2, pp. 897–904, 2011.

[55] T. Majaw, R. Deka, S. Roy, and B. Goswami, "Solar charge controllers using mppt and pwm: A review," *ADBU Journal of Electrical and Electronics Engineering (AJEEE)*, vol. 2, no. 1, pp. 1–4, 2018.

[56] V. Bhan, S. A. Shaikh, Z. H. Khand, T. Ahmed, L. A. Khan, F. A. Chachar, and A. M. Shaikh, "Performance evaluation of perturb and observe algorithm for mppt with buck–boost charge controller in photovoltaic systems," *Journal of Control, Automation and Electrical Systems*, vol. 32, no. 6, pp. 1652–1662, 2021.

[57] A. Mohapatra, B. Nayak, P. Das, and K. B. Mohanty, "A review on mppt techniques of pv system under partial shading condition," *Renewable and Sustainable Energy Reviews*, vol. 80, pp. 854–867, 2017.

[58] D. Yamegueu, Y. Azoumah, X. Py, and H. Kottin, "Experimental analysis of a solar pv/diesel hybrid system without storage: Focus on its dynamic behavior," *International Journal of Electrical Power & Energy Systems*, vol. 44, no. 1, pp. 267–274, 2013.

Appendix A

Plant Model Parameters

Table A.1: Battery Technical Specifications

Parameter	Value	Units
Maximum Capacity	1740	Ah
Cut-off Voltage	337.5	V
Fully Charged Voltage	523.7942	V
Nominal Discharge Current	756.5217	A
Internal Resistance	0.0025862	Ohms
Capacity at Nominal Voltage	1573.5652	Ah
Discharge Current [i1, i2, i3]	[6.5, 13, 32.5]	A

A.1 MATLAB Implementation of EMS algorithm

```
function [P_bat, P_DG, P_net] = EMS(P_pvAvg, P_dem, SOC)
P_ldCrt = 50e0;
P_chrgMax = 500e3;
P_dchrgMax = 500e3;
SOC_max = 95;
SOC_min = 5;

if P_pvAvg > P_ldCrt + P_dem
P_DG = 0;
P_net = P_pvAvg - P_ldCrt - P_dem;
if SOC < SOC_max
P_chrg = max(0, min(P_net, P_chrgMax));
else
P_chrg = 0;
end
else
P_net = P_pvAvg - P_ldCrt - P_dem;
if SOC > SOC_min
P_chrg = -min(abs(P_net), P_dchrgMax);
if abs(P_net) > P_dchrgMax
P_DG = abs(P_net) - P_dchrgMax;
```

```
  else
  P_DG = 0;
  end
  else
  P_chrg = 0;
  P_DG = abs(P_net);
  end
  end
  P_bat = P_chrg;
  end
```

Listing A.1: EMS Function Implementation